PARAMETER OPTIMIZATION OF THE NONLINEAR AND LINEAR XENON OSCILLATION MODELS

by

Vincent J. Mastroianni Jr.

Thesis submitted to the Graduate Faculty of the
Virginia Polytechnic Institute and State University
in partial fulfillment of the requirements for the degree of
MASTER OF SCIENCE
in
Nuclear Science and Engineering

APPROVED:

R. J. Onega, Chairman

J. R. Thomas, Jr.

H. A. Kurstedt, Jr.

May, 1979
Blacksburg, Virginia

ACKNOWLEDGEMENTS

I would like to express my appreciation to my advisor, Dr. R. J. Onega. His patience, guidance, and suggestions made the completion of this work possible.

I would also like to thank Drs. H. A. Kurstedt, Jr. and J. R. Thomas, Jr. for serving on my advisory committee.

Special thanks is owed to Mr. John Teachman. His assistance in the developement of this work was extremely appreciated.

TABLE OF CONTENTS

Chapter I

INTRODUCTION

1.1 BACKGROUND

The object of this work was to develop a linear two-point reactor model from an existing nonlinear model (1) for xenon-135 induced flux oscillations and determine optimum parameters for both models in comparison to actual plant data. A computer simulation was then employed on both models to compare the predictions from these two models against experimental data obtained from Oconee II nuclear power station (2) during start-up testing. A parameter optimization method was utilized on the two models to fit the generated results with one group diffusion theory estimates using a chi-square fit while keeping parameter variations to a 20% limit.

Xenon-135, because of its enormous thermal neutron cross section (2.72E+6 barns) and its relatively large fission yield (0.00237 atoms/fission), is the most significant fission product during operation (3). The production of xenon in reactors which operate with a thermal flux in the range from 10E+12 to 10E+14 n/cm^2 /sec can lead to problems in core stability (4). Xenon is produced as the result of the beta decay of iodine-135 and is also produced directly from fission. The iodine is also produced by fission and by

the decay of tellurium-135. Since the tellurium decays relatively rapidly (half-life of 11 sec) it is possible to assume that all the iodine is produced directly from fission (5,6). The xenon production process is shown below:

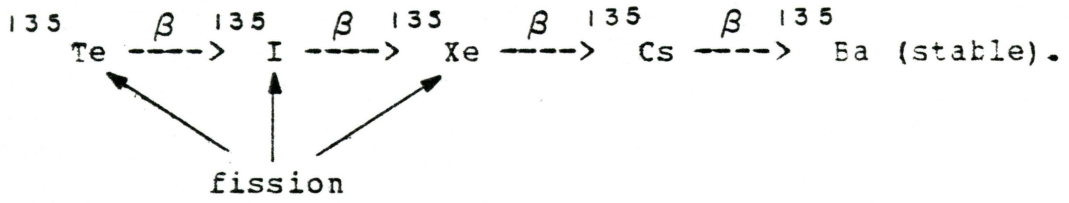

Xenon removal is accomplished through radiative capture (neutron capture) and by radioactive decay. An equilibrium xenon concentration value will be reached when xenon production equals xenon removal during reactor operation. Because xenon has a longer half-life than iodine and since removal of xenon by neutron absorption is lost after reactor shutdown, the peak xenon concentration is obtained hours after reactor shutdown and is dependent upon the operating flux level prior to shutdown. The increased reactivity necessary to overcome this increased concentration of poison is referred to as xenon-override (7) and determines when a reactor re-start is possible. The operating xenon effects (flux oscillations) will be the concern of this work.

During operation under steady-state conditions with a spatially uniform flux, the xenon spatial distribution is uniform and constant with time. Holding the power level constant with an asymmetric flux distribution possibly caused by a perturbation with control rod movement will cause a change in the spatial distribution of xenon. Because xenon loss by neutron capture will decrease in the region of lower flux, the xenon concentration will increase in that region (which will introduce negative reactivity) since the production rate is unchanged due to the iodine concentration before perturbation. Since the total core power level is being held constant, the flux in the opposite region will increase, lowering the xenon concentration and adding positive reactivity.

Large reactor cores can be thought of as several critical masses which are loosely coupled since the neutron migration area is small compared to core size (by a factor of 100 to 1000); this is known as the concept of loosely coupled cores. Operating at high power levels, xenon induced spatial oscillatons are a potential problem in large, loosely coupled reactors (8). Also, the oscillations are more severe for U-235 fueled reactors than for U-233 fueled cores operating under the same conditions (9), because of the smaller production rate of I-135 from U-233

fission. An intermediate behavior would result with cores which contain a mixture of these fissionable isotopes.

Looking at the problem in the axial direction (since this is also the control rod direction) and considering the top and bottom halves as two coupled cores, the flux will oscillate between the two. This is because of the different xenon production and removal rates attributed to the changing flux levels. This process would continue until new equilibrium concentrations of xenon and iodine are reached. Because of the loosely coupled core, the oscillations could possibly become unstable (1,4). A stabilizing influence to balance against the tendency to oscillate is temperature feedback (10). The problems associated with an imbalance in power density range from uneven fuel burn-up to the possibilty of departure from nucleate boiling (1) and clad melting.

During initial start-up and power escalation testing the xenon induced power oscillation measurement is one of the last of the major core transient tests that is conducted (3). A xenon oscillation may be initiated by introducing equal and opposite perturbations in the absorption cross section in the upper and lower halves of the reactor core. This perturbation is accomplished by an insertion and with-

drawal of different control rod banks at the core axial centerline to develop a power offset. Verification that adequate margins exist to the core thermal limits in the presence of the flux peaking in the "overpower" region can then be determined using permanently installed incore neutron detectors.

Computer generated models could help in this area by determining how closely design constraints would be approached. The optimization method developed would aid further in these model predictions since "actual" core parameters instead of one group estimates could be utilized. Safety margins could become less conservative and more realistic. The nonlinear model provided satisfactory results with experimental data using one-group estimates for the parameters. Considerable variation in these estimates were necessary to satisfy the linear model.

1.2 LITERATURE REVIEW

One method of treatment of xenon oscillations is known as modal analysis (8,11). This method involves expansion of the linearized space-dependent kinetics equations by spatial modes and then studying the harmonics. The consideration of xenon instability was next examined (12) and eventually this was extended to include a power-dependent reactivity feedback system (13).

This present work is an extension of the nonlinear model developed by Onega and Kisner (14). Parameter estimation involves assigning values to the unknown parameters in the model on the basis of experimental data. The model is then said to be "validated" if a required accuracy criterion can be satisfied when comparing the model with the plant (15). Since the xenon model is a function of many different nucleonic parameters, methods of variation of these parameters were examined to improve simulation response. The method of maximum likelihood was obtained with a sensitivity analysis performed on only three of these parameters in developing a gradient of the chi-square fit against the actual test data (16).

The complete automation of the simulation and optimization process was the final goal in solving the problem. Methods of optimization that were examined included:

1. One-dimensional search (Powell's method) (17).

2. The Fletcher-Powell method (18).

3. Direct search methods (19).

Methods one and two were disregarded since they involved the application of gradients at each evaluation. These gradients had to be taken with respect to parameters

that were not explicit in the method of problem formulation. This became very difficult to utilize in a computer program working with implicit and integral functions which are inherent to the computer simulation language used, Continuous Simulation Modeling Program (CSMP) (20,21).

The linear equations, or as they are sometimes referred to, the perturbation equations, provide the most common approach to studying the behavior of a nonlinear system in the neighborhood of a known nominal solution, an equilibrium point (22). Linearizing the nonlinear model reduces its complexity but at the same time reduces its applicability to a small region about this equilibrium point. Principal uses for the linearized equations are for investigations of stability, with the main concern being whether the spatial flux oscillation will converge or diverge (23). Both power and spatial oscillations have been studied for different geometries using linearized theory by Canosa (24). Working with the linear equations is not necessarily a trivial task.

1.3 APPROACH

The first question that must be answered in parameter estimation methods is which parameters to vary? Known parameters which are independent of surroundings such as the half-lives of xenon and iodine were eliminated. However

their fission yields were varied since they are functions of neutron energy and are difficult to measure. A total of six parameters were varied since they were considered dependent on operating conditions. Table (I-1) lists the parameters of the system with their initial one-group estimates and denotes the parameters that were varied.

The direct search method selected was the Hooke and Jeeves' method (19). This method is an advanced pattern search method in that it is capable of jumping base points in the direction of the optimization gradient. The method also allows different step sizes for the different parameters to be varied as well as an unlimited number of parameters to vary. The method works just as well for constrained or unconstrained optimization problems.

The nonlinear model (1), along with the sensitivity analysis with respect to six parameters that were chosen to be varied, were written in CSMP. The parameter vector was obtained from a comparison of the experimental flux against the model generated flux using the maximum likelihood method. An algorithm to simulate the Hooke and Jeeves' method was developed, tested, and incorporatd into the main CSMP program. By the selection of initial step sizes for each of the individual parameters, the location of different

TABLE I-1

Model Parameter Values From Oconee II

Parameter	One Group Estimate	Definition
σ_x (cm^2) *	2.72×10^{-18}	Xe cross section
D (cm) *	0.395	Diffusion Coefficient
α ($cm^2 \cdot sec$) *	3.64×10^{-16}	Prompt power feedback
Σ_f (cm^{-1}) *	0.16	Macroscopic fission cross section
γ_x *	0.003	Xe fission yield
γ_i *	0.061	I fission yield
λ_x (sec^{-1})	2.09×10^{-5}	Xe decay constant
λ_i (sec^{-1})	2.87×10^{-5}	I decay constant
$\nu \Sigma_f$ (cm^{-1})	1.56	Neutron production/cm
P MW	2500	Operating power (th)
H (cm)	365.8	Core height
Σ_a (cm^{-1})	1.53	Avg. absorption cross section

* Parameters chosen to be varied

relative minima was possible. The location of the global minimum for the chi-square fit against the test data was also possible. A minimum was considered global if no reduction in this minimum could be found for initial step sizes up to 100% of the initial value. By placing a limit on the maximum variation on a particular parameter, the best relative minimum was determined. Parameter variations were held to 20% of the initial values for the best local minimum. This value was selected since it roughly represents diffusion theory accuracy.

Beginning with the nonlinear equations a linear model was developed. This model was utilized to predict only the response from the perturbation and did not actually incorporate the perturbation. This was accomplished by expanding about an equilibrium point in time just after the perturbation was terminated in the nonlinear model. By analyzing the linear model response using the same procedure as the nonlinear model some questions could be answered. These included:

1. Does the accuracy of the two models differ unreasonably; and if not,

2. Can the linear model be substituted for the nonlinear model in reactor simulation?

Chapter II

MODEL DEVELOPMENT

2.1 BASIC THEORY

A pressurized water reactor (PWR) core may be approximated by a right circular cylinder. Neglecting radial leakage, the cylindrical shape of the PWR core can be modeled by a bare infinite slab. This approximation is validated by including the radial leakage through the radial buckling term into the macroscopic absorption cross section.

Some of the major assumptions that are made in the mathematical development with the slab type core are repeated here (1):

1. A two-point kinetics model can describe the system adequately.

2. Delayed neutrons were considered prompt since their time constant is 2 orders of magnitude less than the xenon buildup time constant.

3. Temperature feedback can be assumed to be in equilibrium and treated as prompt also.

4. The iodine concentration, xenon concentration, and neutron flux spatial shapes can be represented by the sum of the fundamental mode and the first harmonic.

The complete xenon oscillation model would include neutronic as well as the thermal hydraulic effects. The thermal effects, considered prompt (assumption 3), are lumped through the prompt power feedback parameter, α .

The method for comparison of the model generated data against plant data was developed as follows; the experimentally measured flux was compared against the model generated flux at each instant in time during simulation to obtain estimates of the chi-square. This chi-square was found by (25)

$$\chi^2 = \sum \frac{(\text{Observed}-\text{Expected})^2}{\text{Expected}} . \qquad (2.1)$$

A parameter vector was formed to be utilized in the sensitivity equations (parameters were defined in Table I-1),

$$\vec{\theta} = \left[\theta_1, \theta_2, \ldots, \theta_6\right]^T , \qquad (2.2)$$

where

$$\theta_1 = \sigma_x / \sigma_x^\circ \quad , \tag{2.3}$$

$$\theta_2 = D / D^\circ \quad , \tag{2.4}$$

$$\theta_3 = \alpha / \alpha^\circ \quad , \tag{2.5}$$

$$\theta_4 = \Sigma_f / \Sigma_f^\circ \quad , \tag{2.6}$$

$$\theta_5 = \gamma_x / \gamma_x^\circ \quad , \tag{2.7}$$

and

$$\theta_6 = \gamma_1 / \gamma_1^\circ \quad . \tag{2.8}$$

The superscript indicates the original values of the parameter obtained from Oconee II.

Originally the method developed by Onega (16) for finding the gradient of the chi-square fit was intended to be used. A very brief description of this method and why it could not be utilized is given in Appendix A.

2.2 NONLINEAR MODEL

The nonlinear xenon oscillation model is described in detail in the literature (1,14). To establish a starting point for notation, the time varying amplitudes of the normalized flux, xenon, and iodine concentrations respectively were expressed as

$$\psi(z,t) = \cos(bz) + A(t)\sin(2bz) , \qquad (2.9)$$

$$x(z,t) = \cos(bz) + B(t)\sin(2bz) , \qquad (2.10)$$

and

$$y(z,t) = \cos(bz) + C(t)\sin(2bz) . \qquad (2.11)$$

The PWR core is treated in slab geometry and represented by two points and $b = \pi/H$.

The product of the peak steady-state values of the flux, xenon, and iodine concentrations and their time varying amplitudes were respectively represented as

$$\phi(z,t) = \phi_o\psi(z,t) , \qquad (2.12)$$

$$X\ (z,t) = X_o\ x(z,t)\ , \tag{2.13}$$

and

$$I\ (z,t) = I_o\ y(z,t)\ . \tag{2.14}$$

The coefficients of the first harmonic A(t), B(t), and C(t) were obtained by integrating over the two halves of the core. The xenon and iodine differential equations in terms of these coefficients and in terms of the elements of the parameter vector are

$$\frac{dB}{dt} = \left[\gamma_x \Sigma_f \frac{\Phi_o}{X_o}\right] A(t) + \left[\lambda_1 \frac{I_o}{X_o}\right] C(t) - \lambda_x B(t) - (\sigma_x \phi_o)\ (2/3\ (A + B) + \pi/4\ A\ B)\ , \tag{2.15}$$

and

$$\frac{dC}{dt} = \left[\gamma_1\ \Sigma_f \frac{\Phi_o}{I_o}\right] A(t) - \lambda_1\, C(t)\ . \tag{2.16}$$

where I_o and X_o are the peak steady-state values for the iodine and xenon concentrations resepctively. The steady

state flux Φ_o was determined from the operating power level. The other parameters are defined in Table (I-1).

The expansion coefficient for the flux can be determined from the diffusion equation and after some algebraic manipulation is expressed as

$$A(t) = v - \sqrt{v^2 + 1} \tag{2.17}$$

where

$$v = \frac{(45\pi^3/8H^2D - X_o\sigma_x + 7\phi_o\alpha\Sigma_a)}{(8X_o\sigma_x\ B(t))} . \tag{2.18}$$

The system sensitivity equations, which represent how sensitive the dependent variables A(t), B(t), and C(t) are to a change in a particular parameter θ_j, are

$$\partial A/\partial\theta_j = f_{Aj}(A(t), B(t)) \qquad j=1,2,\ldots,6 , \tag{2.19}$$

$$\partial B/\partial\theta_j = f_{Bj}(\partial A/\partial\theta_j , \partial B/\partial\theta_j , \partial C/\partial\theta_j , A(t), B(t)) , \tag{2.20}$$

and

$$\partial C/\partial \theta_j = f_{cj}(\partial A/\partial \theta_j \ , \partial C/\partial \theta_j) \ . \qquad (2.21)$$

The complete equations are listed in Appendix B.

2.3 LINEAR MODEL

Beginning with Eqs. (2.15 - 2.17), the linear model was developed by first substituting A(t) into Eqs. (2.15) and (2.16). This was done to reduce the equations to functions of B(t) and C(t). Rewriting A(t) with Eq. (2.18) substituted for v, i.e. going back to the original variables, gives

$$A(t) = \frac{e1 - \sqrt{e1^2 + e4\ B(t)^2}}{e6\ B(t)} \qquad (2.22)$$

where

$$e1 = \beta_1 - \beta_3 \ , \qquad (2.23)$$

$$e4 = \left[(64/15\pi\ \sigma_x\ X_o)/\ \Sigma_f\right]^2 \ , \qquad (2.24)$$

$$e6 = (64/15\pi\ \sigma_x\ X_o)/\ \Sigma_f \quad , \tag{2.25}$$

$$\beta_1 = \left[\ 4Db^2 + .5(\Sigma_{a1}+\Sigma_{a2}) + 32/15\pi\ (\sigma_x X_o + 3\alpha\phi_o\Sigma_a)\right]/\ \Sigma_f \quad , \tag{2.26}$$

and

$$\beta_3 = \left[\ Db^2 + .5(\Sigma_{a1}+\Sigma_{a2}) + 8/3\pi\ (\sigma_x X_o + \alpha\phi_o\Sigma_a)\right]/\ \Sigma_f \quad . \tag{2.27}$$

The constants named above correspond to their definitions in the actual computer program. Substituting Eq. (2.22) into Eqs. (2.15) and (2.16) gives

$$\frac{dC}{dt} = \frac{c11(e1 - \sqrt{e1^2 + e4\ B(t)^2})}{e6\ B(t)} - \lambda_1 C(t) \quad , \tag{2.28}$$

and

$$\frac{dB}{dt} = b12\ C(t) - (\lambda_x + 2/3\ b14)\ B(t)$$

$$+ \frac{(b11 - 2/3\ b14 - \quad /4\ b11\ B)\ (e1 - \sqrt{e1^2 + e4\ B^2})}{e6\ B(t)}, \tag{2.29}$$

where

$$b11 = (\gamma_x \Sigma_f\ \phi_o\ / X_o) \tag{2.30}$$

$$b12 = (\lambda_1\ I_o / X_o) \tag{2.31}$$

$$b14 = (\sigma_x\ \phi_o) \tag{2.32}$$

$$c11 = (\gamma_1\ \Sigma_f \phi_o / I_o)\ . \tag{2.33}$$

The algebraic manipulations performed above on the nonlinear model made this system of equations suitable for linearizing by eliminating A(t). One of the most useful formulas in the analysis of nonlinear equations is the Taylor series expansion (22). The Taylor expansion of a function of two variables B and C is

$$f(B_o+\Delta B, C_o+\Delta C) = f(B_o, C_o) + \left.\frac{\partial f}{\partial B}\right|_o \Delta B + \left.\frac{\partial f}{\partial C}\right|_o \Delta C + \frac{1}{2!}\left.\frac{\partial^2 f}{\partial B^2}\right|_o \Delta B^2 + \cdots \quad (2.34)$$

It is normal in perturbation theory analysis (22) to eliminate all terms higher than first-order and reduce Eq. (2.34) to

$$f(B_o+\Delta B, C_o+\Delta C) = f(B_o, C_o) + \left.\frac{\partial f}{\partial B}\right|_o \Delta B + \left.\frac{\partial f}{\partial C}\right|_o \Delta C \quad (2.35)$$

Now B(t) and C(t) are represented by

$$B(t) = B + \Delta B(t) \quad (2.36)$$

and

$$C(t) = C_o + \Delta C(t) \quad . \tag{2.37}$$

Following this procedure the linearized forms of Eqs. (2.28 and 2.29) became

$$\frac{d\Delta C}{dt} = \frac{-c11 \cdot e1 (e1^2 + e4\ B_o^2) + c11 \cdot e1^2}{e6\ B_o (e1 + e4\ B_o)}\ \Delta B - \lambda_1 \Delta C + \left.\frac{dC}{dt}\right|_o \tag{2.38}$$

and

$$\frac{d\Delta B}{dt} = b12\,\Delta C - (\lambda_x + 2/3\ b14)\,\Delta B - \left[\frac{(b11 - 2/3\ b14 - \pi/4\ b14\ B_o)\ e4}{e6\,(e1^2 + e4\ B_o^2)^{1/2}} - (e1^2 + e4\ B_o^2)\ \frac{(b11 - 2/3\ b14)}{e6\ B_o^2}\right]\Delta B - \frac{(b11 - 2/3\ b14)\,e1}{e6\ B_o^2}\ \Delta B + \left.\frac{dB}{dt}\right|_o \tag{2.39}$$

Since the solution of the linearized concentrations are in effect oscillating around B_o and C_o it was imperative that these constants are evaluated correctly. B_o and C_o were found by setting Eqs. (2.28) and (2.29) equal to zero. These values were found to equal zero for the steady-state homogeneous case. This was the expected result since for a uniform and unperturbed core the only possible spatial distribution is a pure cosine.

A quick way of determining if A_o, B_o, C_o, and $A(t)$, $B(t)$, and $C(t)$ were reasonable was that they must lie in the interval from -1 to $+1$ to keep a positive spatial distribution in Eqs. (2.9 - 2.11). The zero solution for the steady state values was the only solution that was in this interval.

The nonlinear computer model simulation began at time zero and lasted to time 53.5 hours. The perturbation was initiated at time 10.0 hours and lasted for 2.5 hours while normal operation was simulated from time zero to the time that the perturbation was initiated to assure that steady state conditions were satisfied. However the linear model had to be started at time 12.5 hours, just after the perturbation was terminated. With the zero steady state conditions the linear model computer simulation would diverge for

all time except during the time of the perturbation since the linear model as written had the difference of the absorption cross sections plus B_o in the denominator, which of course would be zero. The values of A(t), B(t), and C(t) at time 12.5 hours obtained from the nonlinear model were utilized in the linear model as initial conditions. Initial conditions on the integrals compensated for the difference in the nonlinear A(t) and the linear A_o at 12.5 hours. To incorporate in the linear model program the ability of dividing by zero would more than double the size of the program and increase running time substantially.

Initial conditions for the $\Delta B(12.5)$ and $\Delta C(12.5)$ were found from rearranging Eqs. (2.36) and (2.37) for time 12.5 hours:

$$\Delta B(12.5) = B(12.5) - B_o = B(12.5) \qquad (2.40)$$

and

$$\Delta C(12.5) = C(12.5) - C_o = C(12.5). \qquad (2.41)$$

The sensitivity analysis was next performed for comparison purposes in the same manner as was done to the nonlinear model except now A(t) was eliminated explicitly from the system. These equations are presented in Appendix C.

A description of the Hooke and Jeeves' method is presented in Appendix D. This optimization method was very compatible for programming and was easily applied to the problem since it allowed different step sizes for the different parameters being varied.

Chapter III

SIMULATION RESULTS

3.1 BACKGROUND

The Oconee reactor had been operating at 75% of full power at equilibrium conditions prior to perturbation. The average thermal flux at this power level was calculated to be 2.0E+13 n/cm^2 /sec. A sequence of rod movements was initiated to induce axial xenon oscillations while deboration was used to maintain criticality. Control rods were returned to their original positions 2.5 hours later. A reactivity change of 0.18% $\Delta K/K$ had resulted due to the rod movement. The reactivty change was translated into an overall absorption cross section by boron addition. Boron concentration calculations indicated the 0.18% $\Delta K/K$ was equivalent to a 0.25% change in absorption cross section. The normalized oscillation produced at the plant is shown in Fig. (III-1).

The CSMP model developed was executed on the Virginia Tech computer system consisting of an IBM 370/158. A rectangular pulse equivalent to a 0.25% change in absortion cross section and lasting for 2.5 hours was used to initiate the oscillations. The 0.25% change was used to also remain consistent with the nonlinear model developed (1).

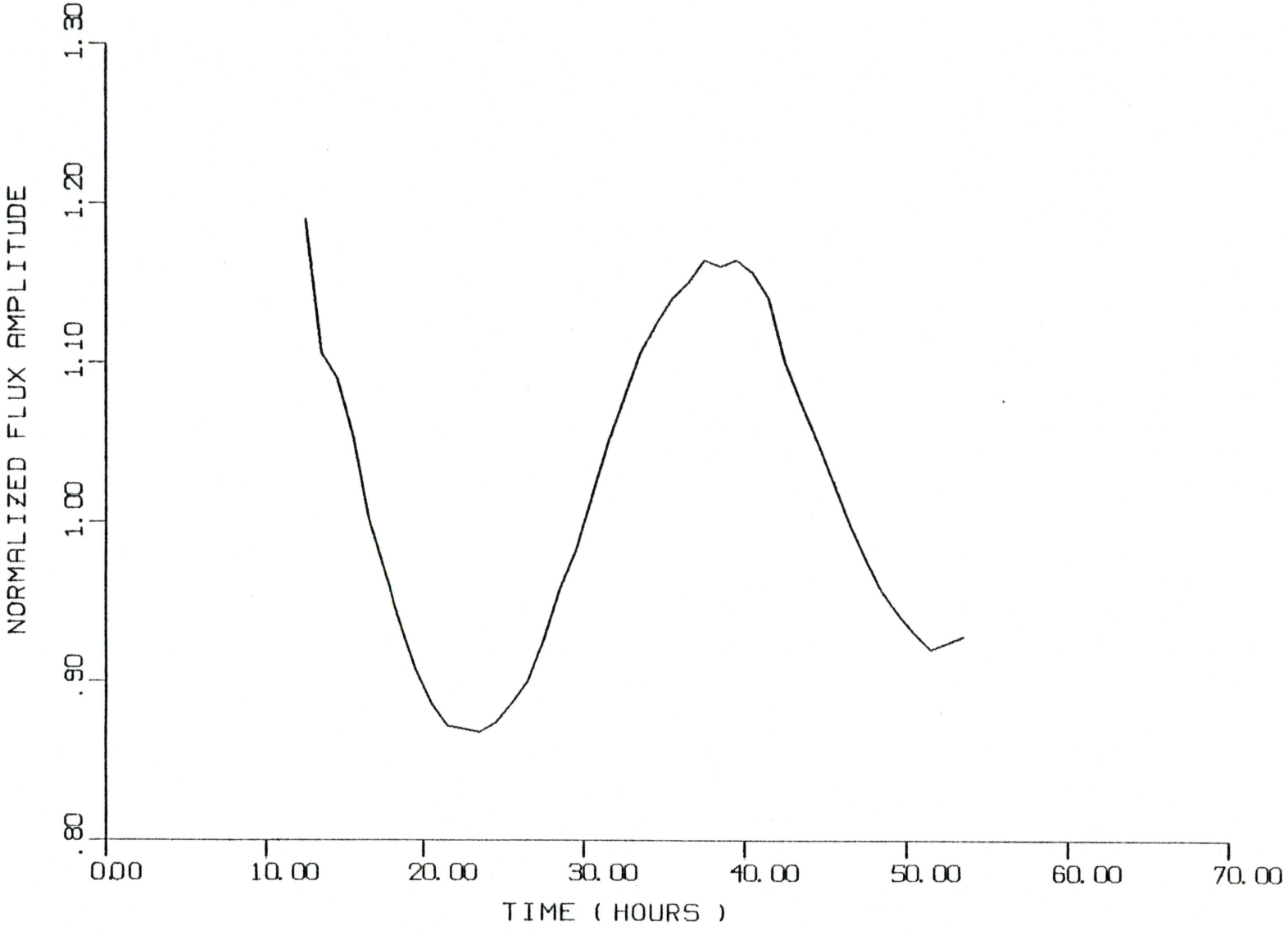

Fig. III-1 ACTUAL PLANT OSCILLATION

3.2 NONLINEAR MODEL RESULTS

The nonlinear model produced extremely good results with a chi-square fit of 0.7082 using diffusion theory estimates. This value could only be reduced to 0.6951 through optimization for the best local minimum. However, even when the global minimum was searched for, the same optimum point was established. As can be seen from Table (III-1) the initial step sizes for the individual parameters were quite large when searching for the global minimum. The same minimum was accomplished with step sizes of 1/100 of those listed in Table (III-1), confirming the possibility of this minimum being global. These results indicate that the initial diffusion parameter estimates are very good.

However, in keeping with the criterion of only allowing a 20% maximum change from diffusion theory estimates in any particular parameter, there is a difference between this global minimum found and the local minimum that is required. Holding γ_x to a maximum 20% change produced a fit of 0.6995 and did not result in changes for the other optimum values listed in Table (III-1).

Figure (III-2) shows a comparision of the nonlinear model results calculated using the initial one group diffusion theory estimates against the actual plant oscillation.

TABLE III-1

Nonlinear Model Optimum Values for Global Minimum

Parameter	Initial Step Size	Optimum Value	% Change
$\sigma_x \times 10^{18}$ (cm^2)	0.5	2.72	0.0
D (cm)	0.05	0.405	2.5
$\alpha \times 10^{16}$ $(cm^2 \cdot sec)$	0.5	3.64	0.0
Σ_f (cm^{-1})	0.05	0.14	12.5
γ_x	0.0005	0.0046	53.0
γ_1	0.005	0.061	0.0

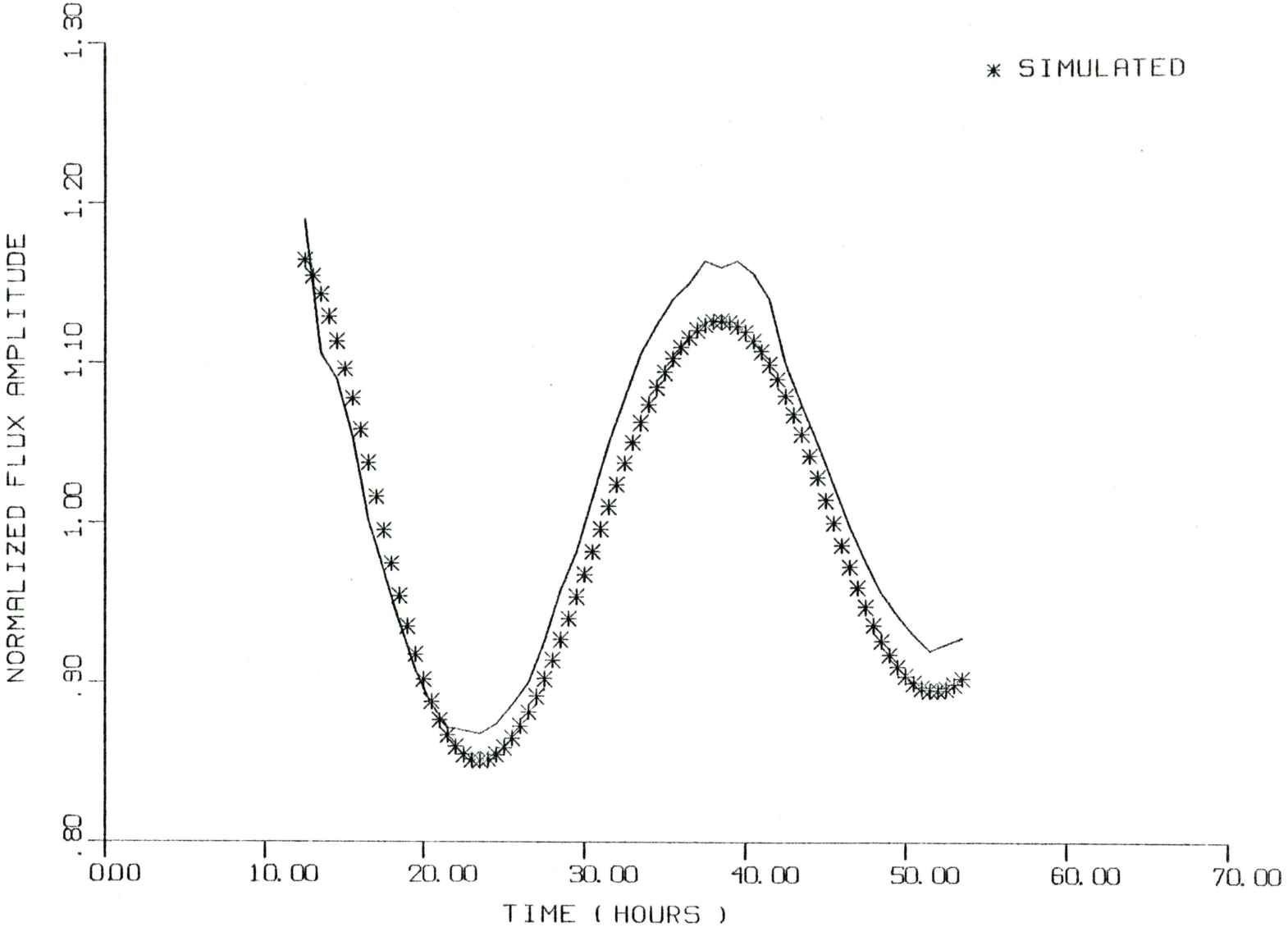

Fig. III-2 INITIAL NONLINEAR FIT

Figure (III-3) is a comparison the actual plant data against the globally optimized nonlinear model. There is no drastic difference in the two figures since their was not much difference in the parameters used between the two simulations. The noticeable difference is that the peak at 37 hours is centered for the optimum simulation.

Plots of the sensitivity equations, which are given in Appendix B, are presented in Figs. (III-4 to III-9). As can be seen from Fig. (III-4) the nonlinear model is predominantly sensitive to changes in σ_x because of the wide variation of $\partial B(t)/\partial\theta_j$. In fact, because of the initially low chi-square fit and the high sensitivity of the model to this parameter it did not have to be changed for optimization. At the optimum values, a 0.5% increase in the xenon cross section resulted in a 0.6% increase in the associated chi-square fit.

It must be stated at this time that the simulated results were not corrected for offset as was done in previous work (1). The correct offset was 1.03 or 3% of what was utilized. This is the only correct method that can be used for general simulation purposes since the model will be utilized to predict responses for perturbations that occur in the core during operation. The purpose of this work was to

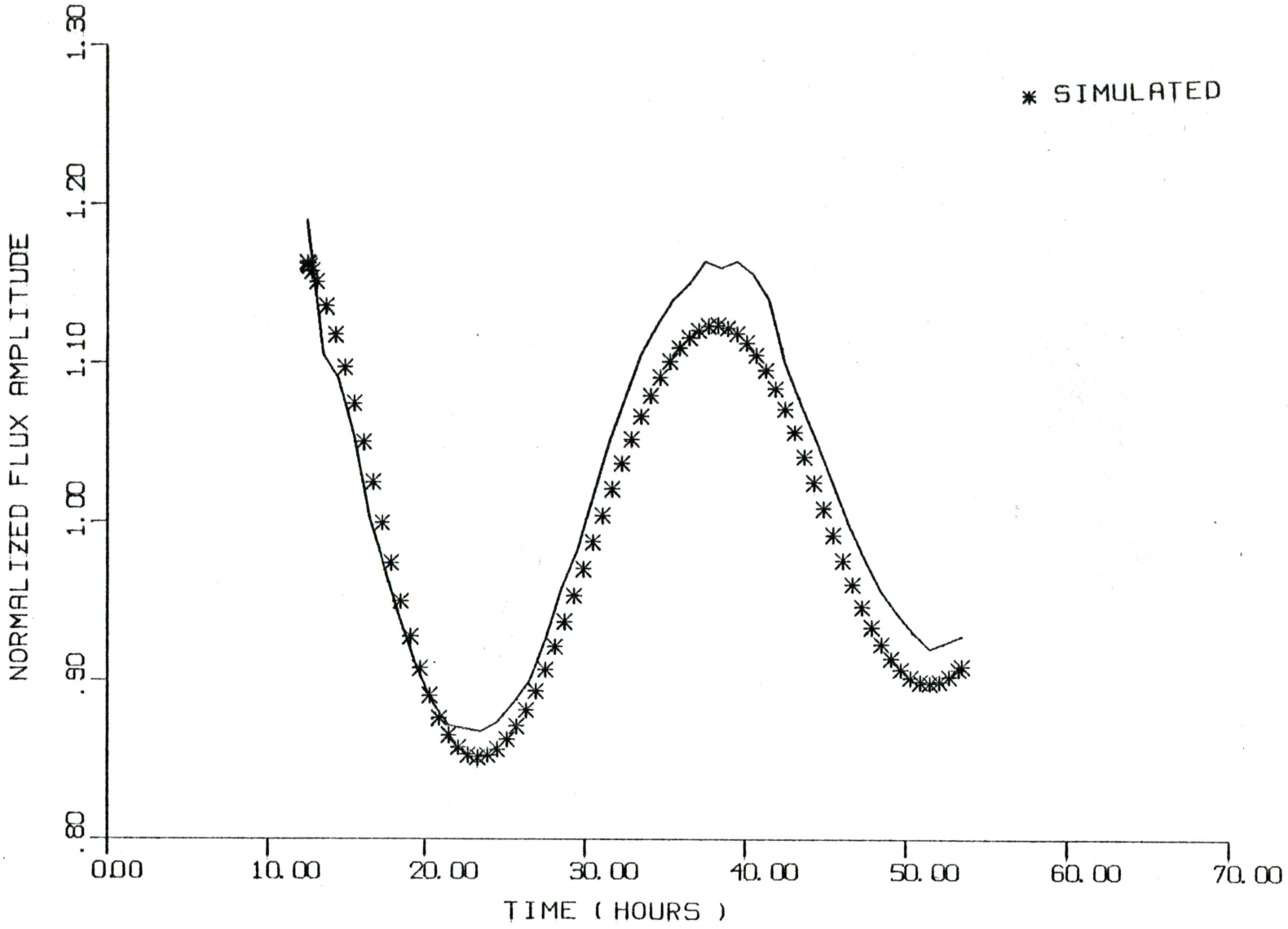

Fig. III-3 OPTIMUM NONLINEAR FIT

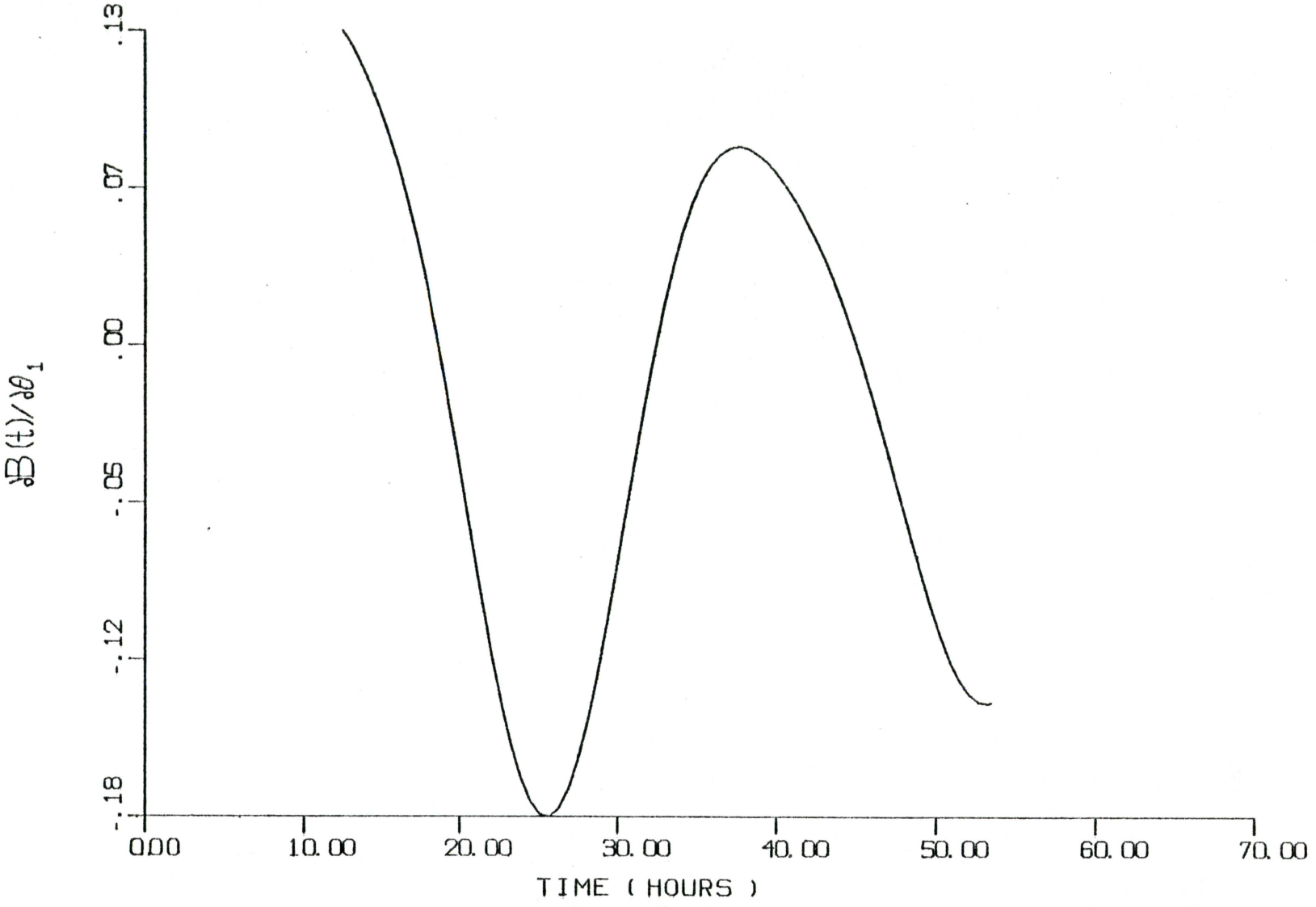

Fig. III-4. SENSITIVITY ANALYSIS OF σ_x

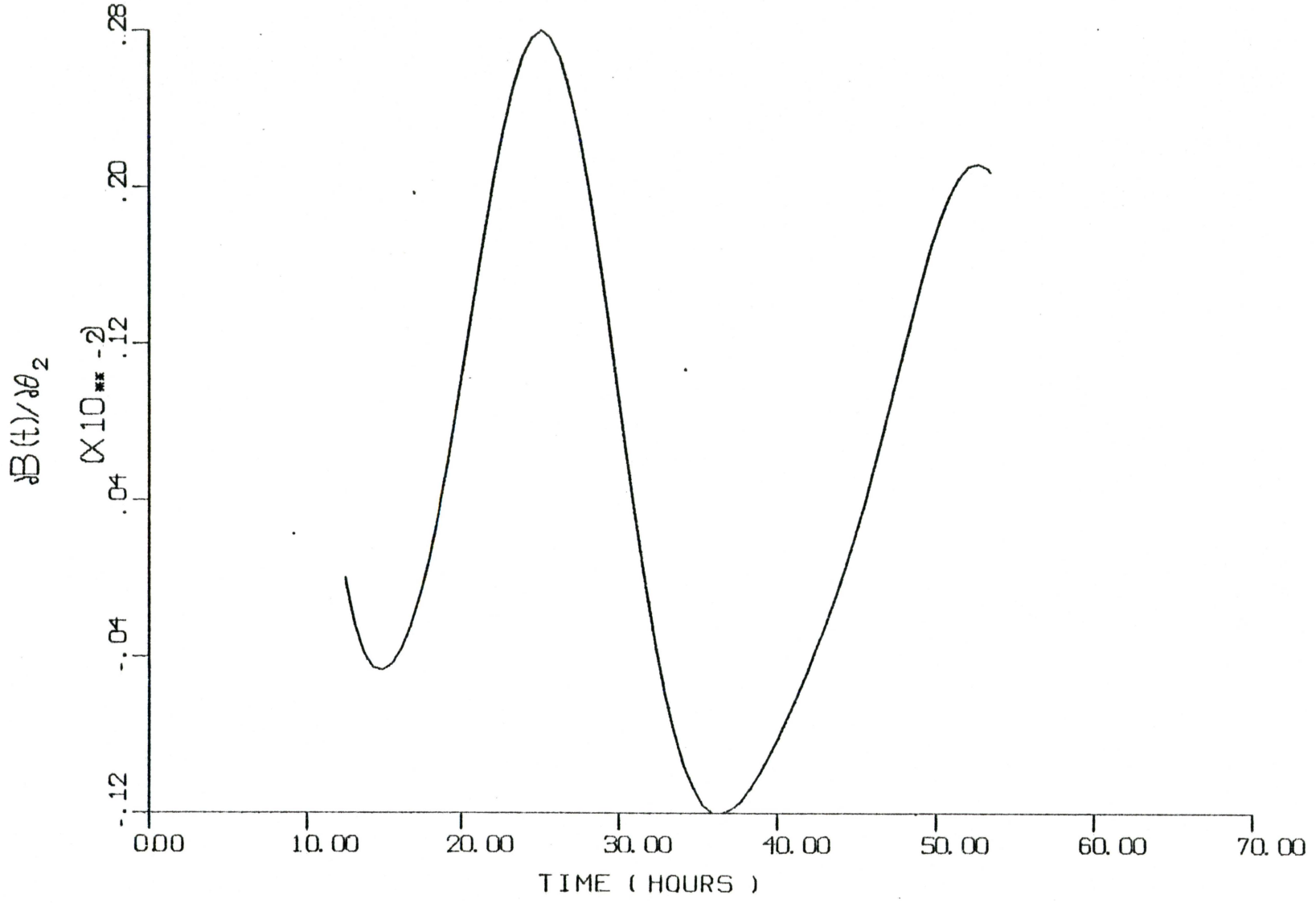

Fig. III-5. SENSITIVITY ANALYSIS OF D

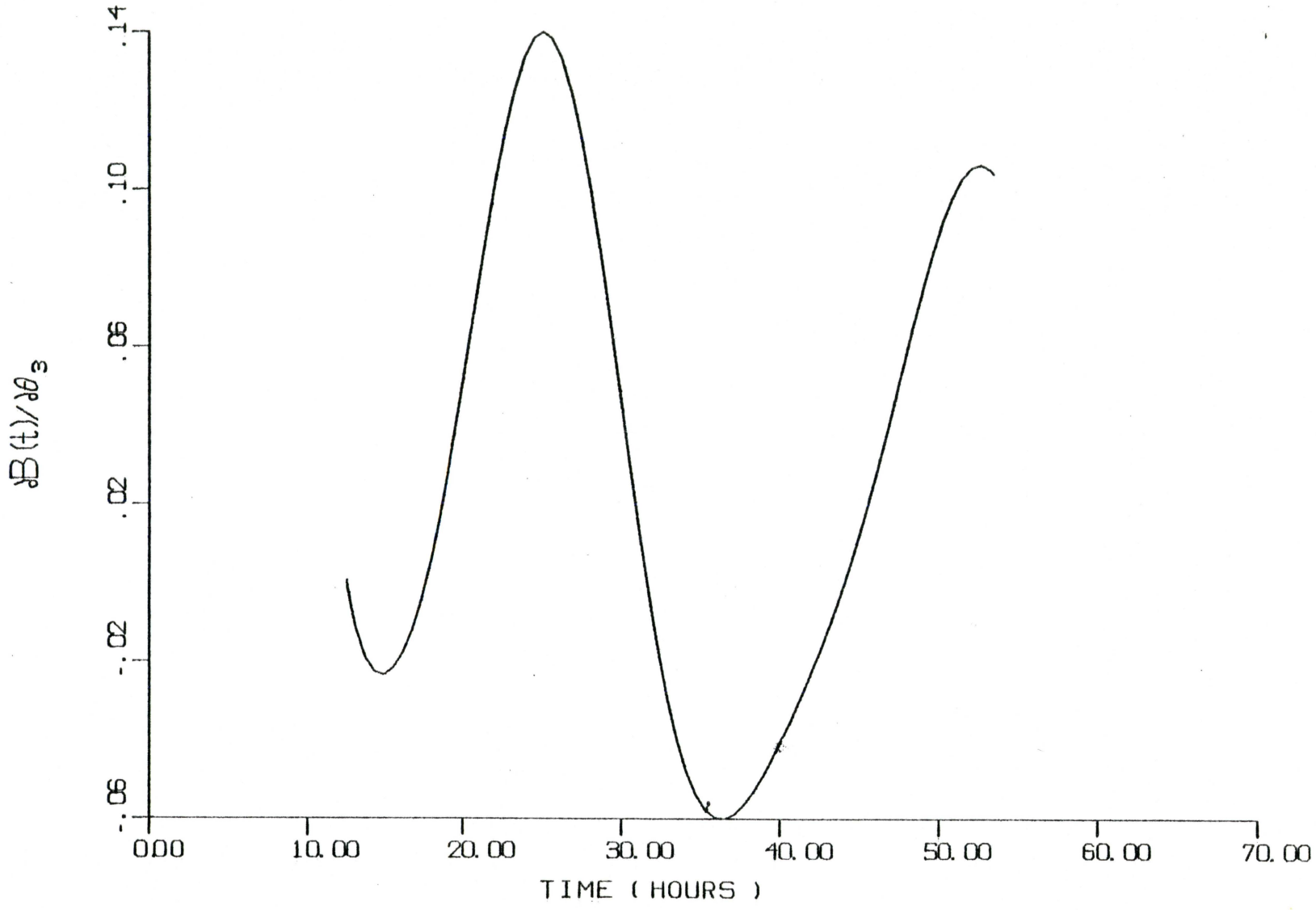

Fig. III-6. SENSITIVITY ANALYSIS OF α

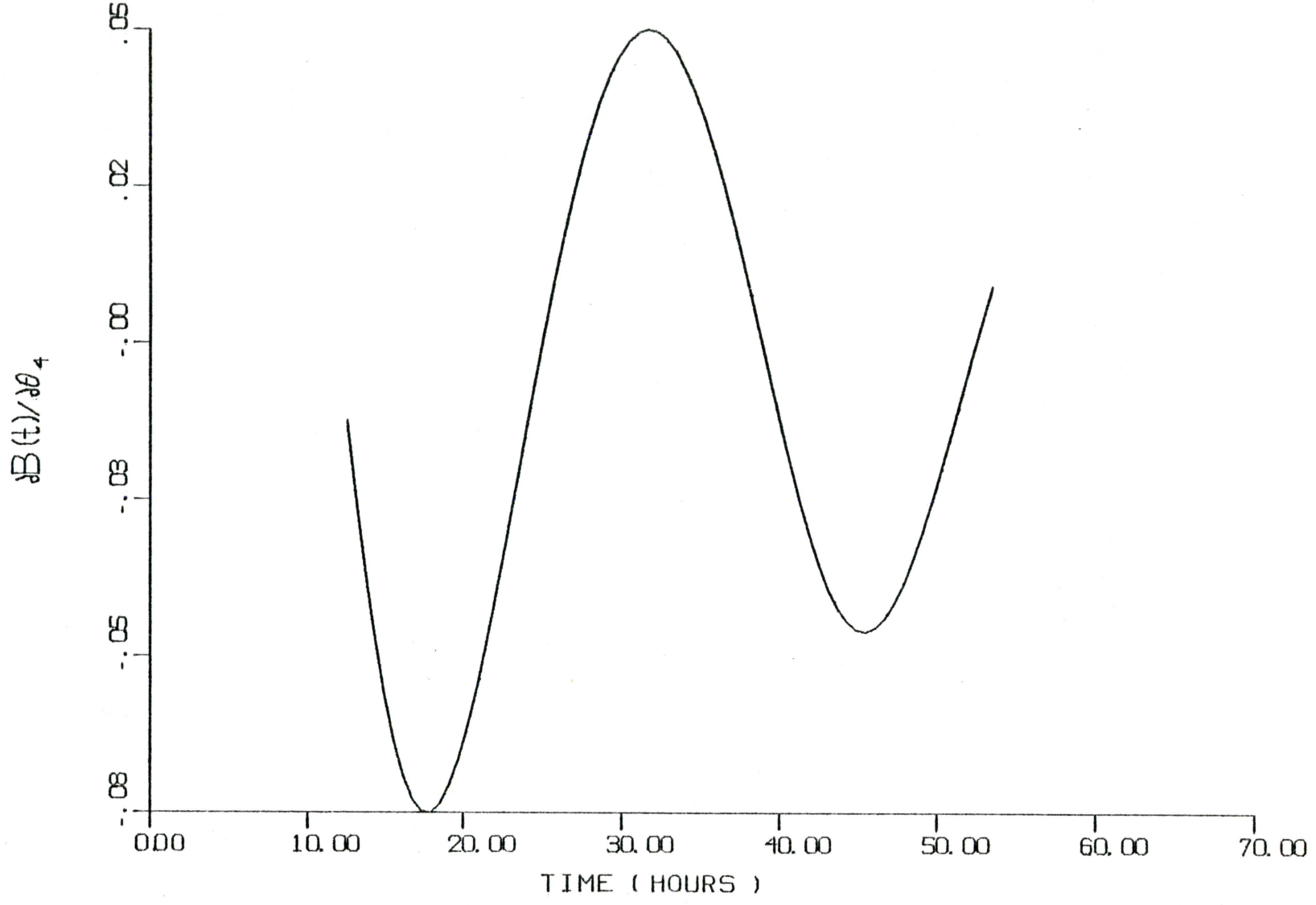

Fig. III-7. SENSITIVITY ANALYSIS OF Σ_f

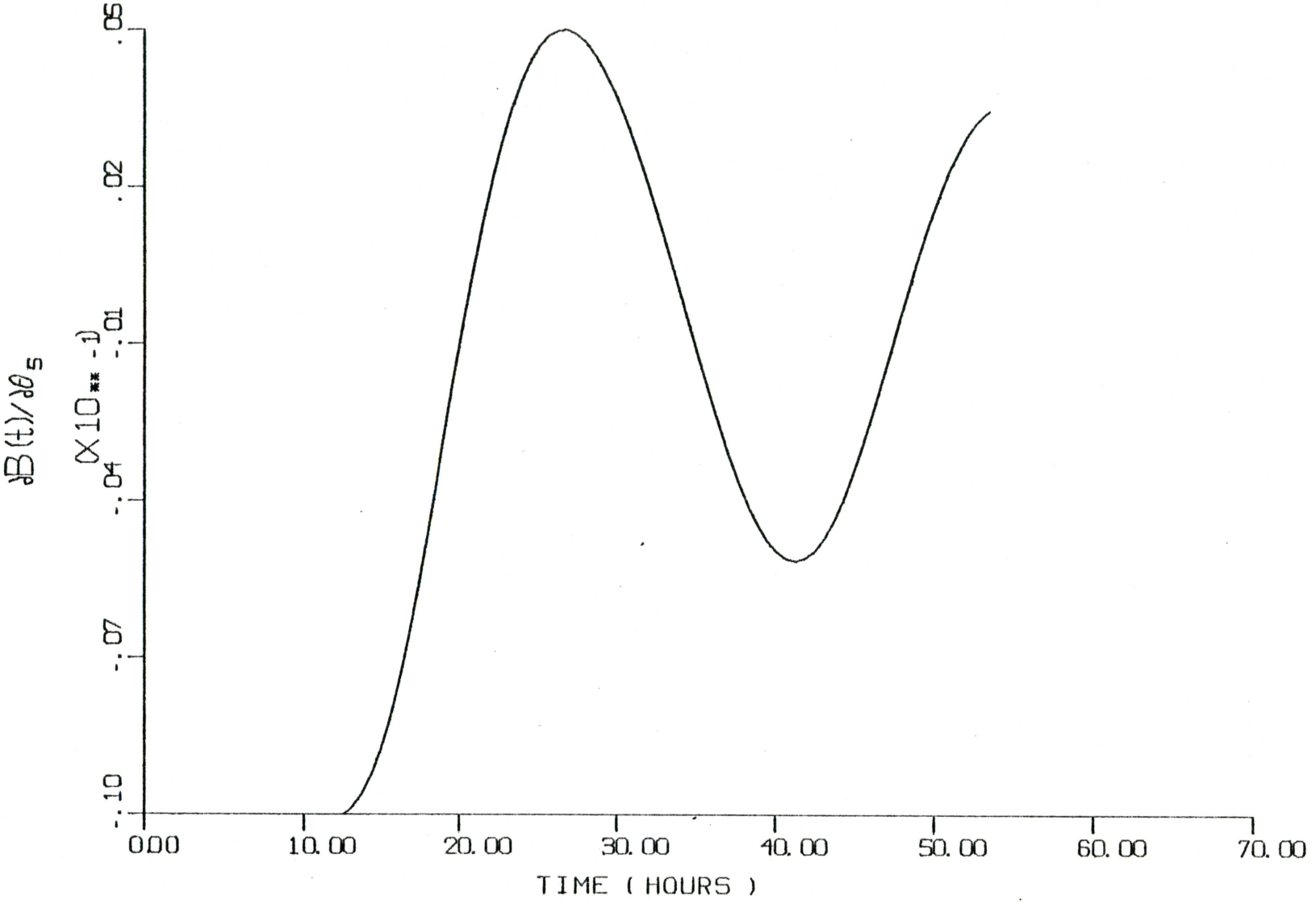

Fig. III-8. SENSITIVITY ANALYSIS OF γ_x

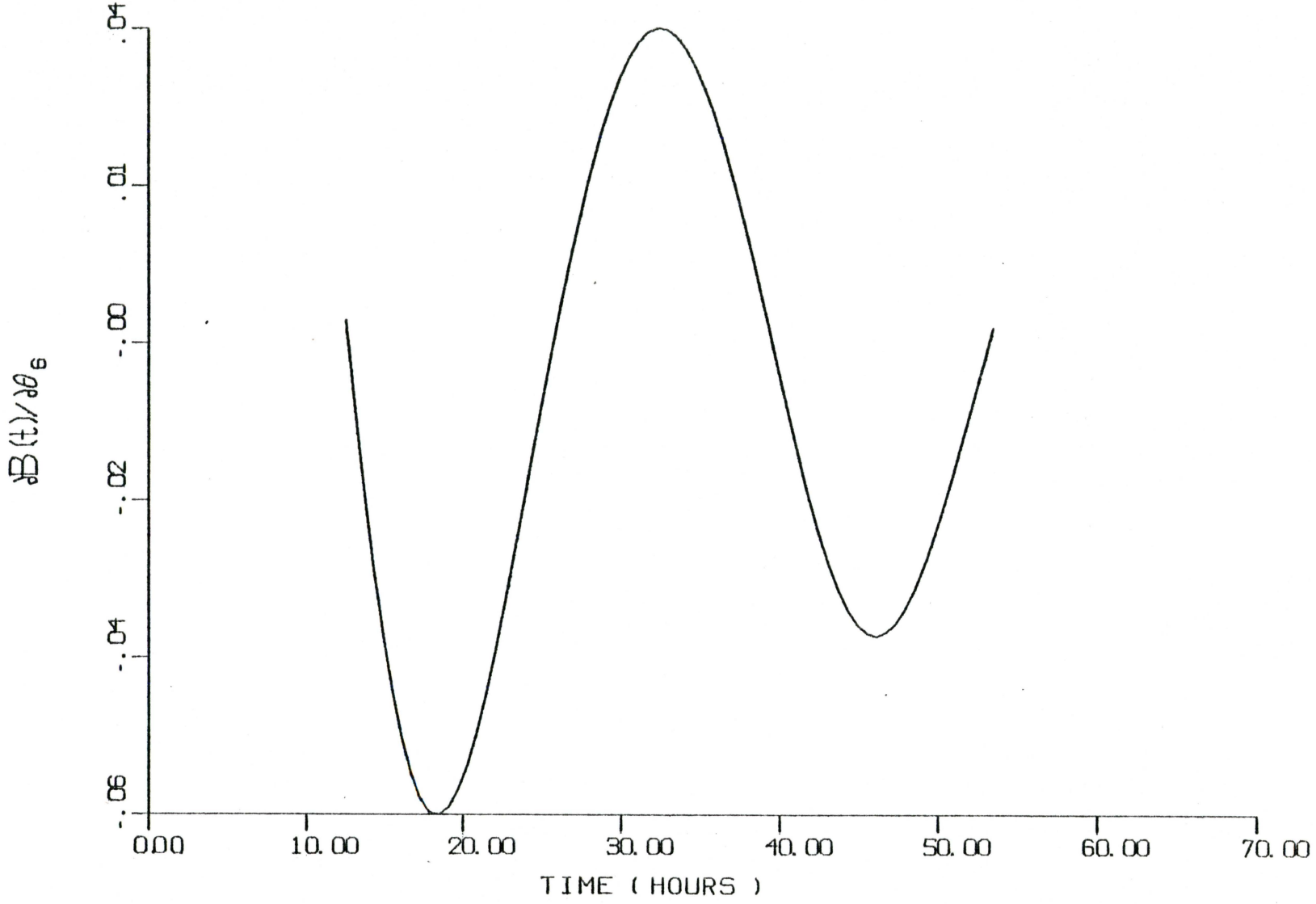

Fig. III-9. SENSITIVITY ANALYSIS OF γ_I

match the actual data by varying nucleonic parameters. If the nonlinear model is to be used to simulate a particular plant with a known offset, then the offset can be incorporated into the model. In fact, the particular offset only has to be added to the results before they are outputted.

The value of α represents a negative power feedback coefficient. Negative power feedback limits local power peaking and stabilizes the system to produce a converging oscillation (23). Since the initial amplitude of the oscillation matched the experimental data very well, again not considering offset, the feedback parameter α did not vary from its initial estimate. As can be seen from Fig. (III-6) the feedback term is the second most sensitive parameter to the nonlinear model.

The period of the optimum model was decreased 2% for an improved fit against plant data. This was accomplished through a 53% increase in the rate of production of xenon atoms from fission. However at the same time the macroscopic fission cross section was reduced 12.5% and the diffusion coefficent increased 2.5% to increase neutron leakage. Because of the increased leakage, the rate of xenon production changed drastically to produce a change in response since the model was not sensitive to the xenon production term as can be noted from Fig. (III-8).

This work supports the analysis presented by Kisner (1) since his parameters differ little from the optimized model. One parameter σ_x , which was not varied in that anaylsis, just happens to be the most sensitive in the nonlinear model. The nonlinear model was run at the optimum parameters with σ_x varying in 4% increments to determine stability. The model was stable for all values below 2.72E+6 barns and up to 3.02E+6 barns. At 3.02E+6 barns the model produced an undamped oscillation while values above this produced diverging oscillations for the optimized parameters.

3.3 LINEAR MODEL

Solving Eqs. (2.25) and (2.26) for the steady-state conditions produced

$$A_o = 0.0 \quad ,$$

$$B_o = 0.0 \quad ,$$

and

$$C_o = 0.0 \quad .$$

From the nonlinear model the coefficients for the initial simulation at time 12.5 were

$$A(12.5) = -0.1645 \quad ,$$

$$B(12.5) = 0.0890 \quad ,$$

and $C(12.5) = -0.0661$.

The initial conditions for the linear model were determined from Eqs. (2.40) and (2.41) and were found to be

$$\Delta A(12.5) = -0.1645 ,$$

$$\Delta B(12.5) = 0.0890 ,$$

and $$\Delta C(12.5) = -0.0661 .$$

The initial simulation of the linear model, with the one group diffusion estimates, produced a slightly diverging oscillation as shown in Fig. (III-10). The amplitude of this oscillation was, however, approximately three times too large and the period was increased 18%. The chi-square fit of this result was 36.24. Through parameter optimization, the best chi-square fit, while keeping parameter variation to a maximum 20% change, was 3.53. Table (III-2) lists these constrained optimized parameters while the response produced is shown in Fig. (III-11). Figures (III-12 to III-17) show the sensitivity analysis of the linear model at this local optimum point.

In continuing the optimization process for a reduction in this minimum, the xenon and iodine production terms were

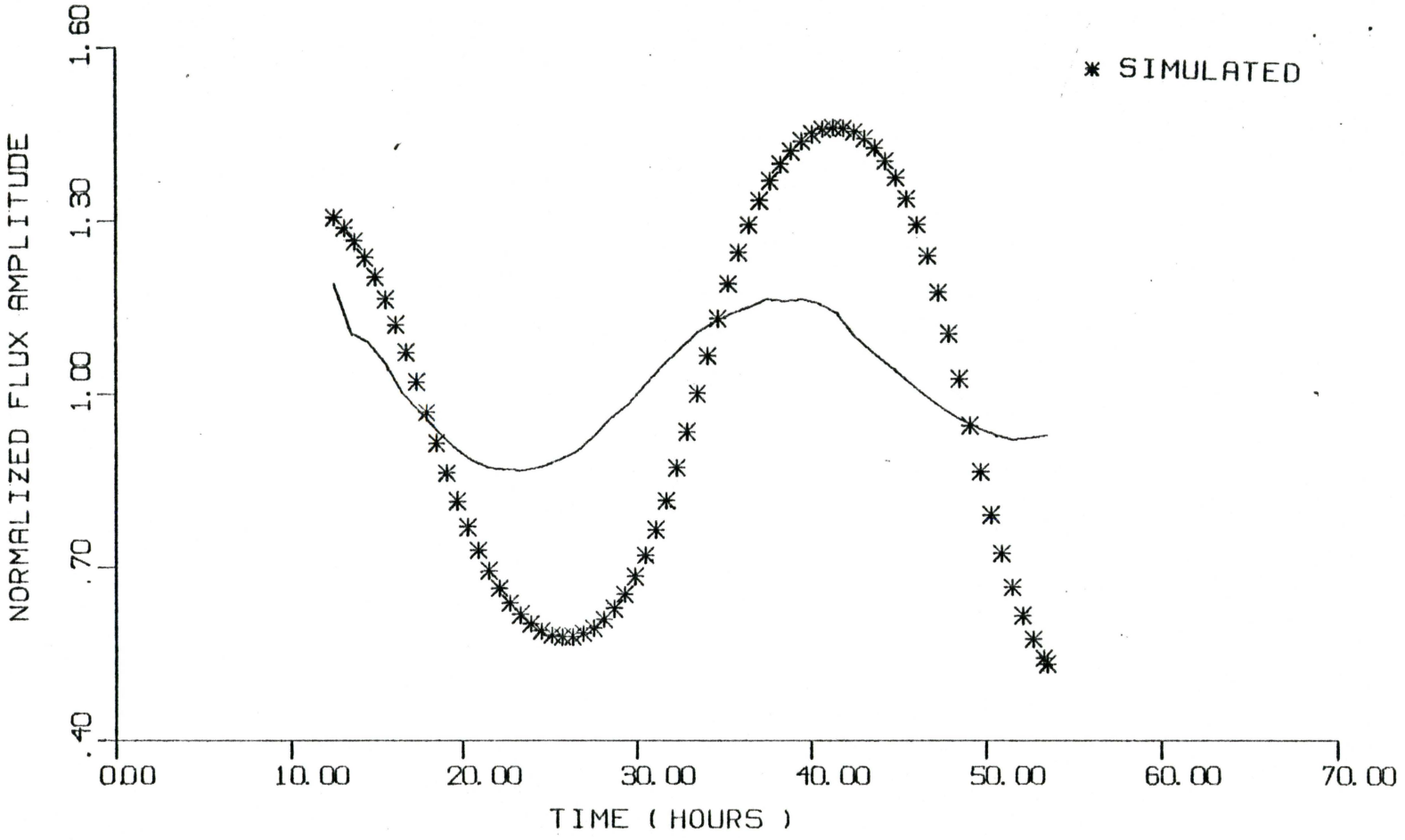

Fig. III-10 INITIAL LINEAR FIT

TABLE III-2

Linear Model Optimum Values

Parameter	Optimum Value	% Change
$\sigma_x \times 10^{18}$ (cm^2)	2.645	2.8
D (cm)	0.405	2.5
$\alpha \times 10^{16}$ $(cm^2 \cdot sec)$	3.652	0.3
Σ_f (cm^2)	0.135	15.6
γ_x	0.0024	20.0
γ_1	0.0488	20.0

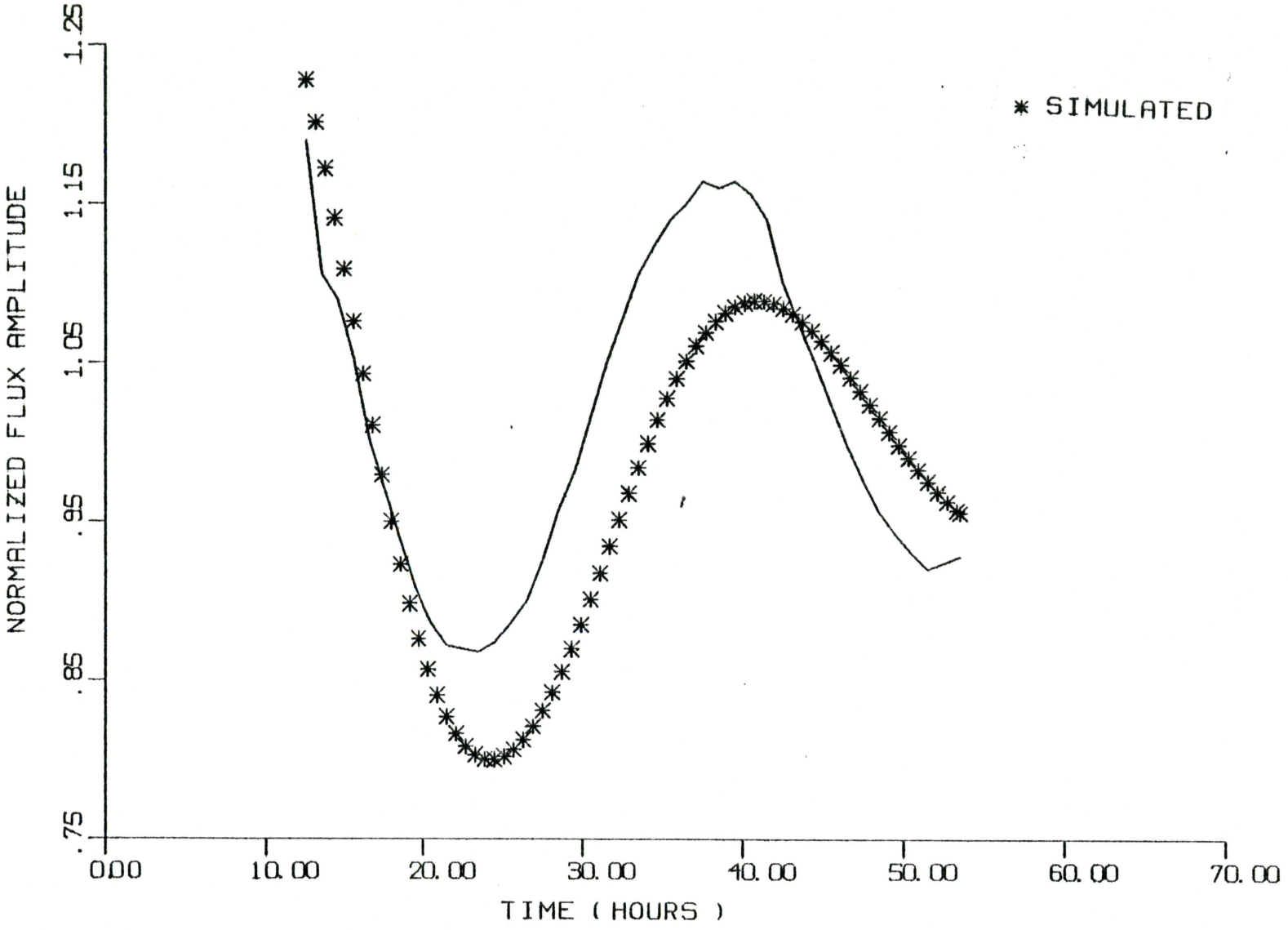

Fig. III-11 OPTIMUM LINEAR FIT (LOCAL)

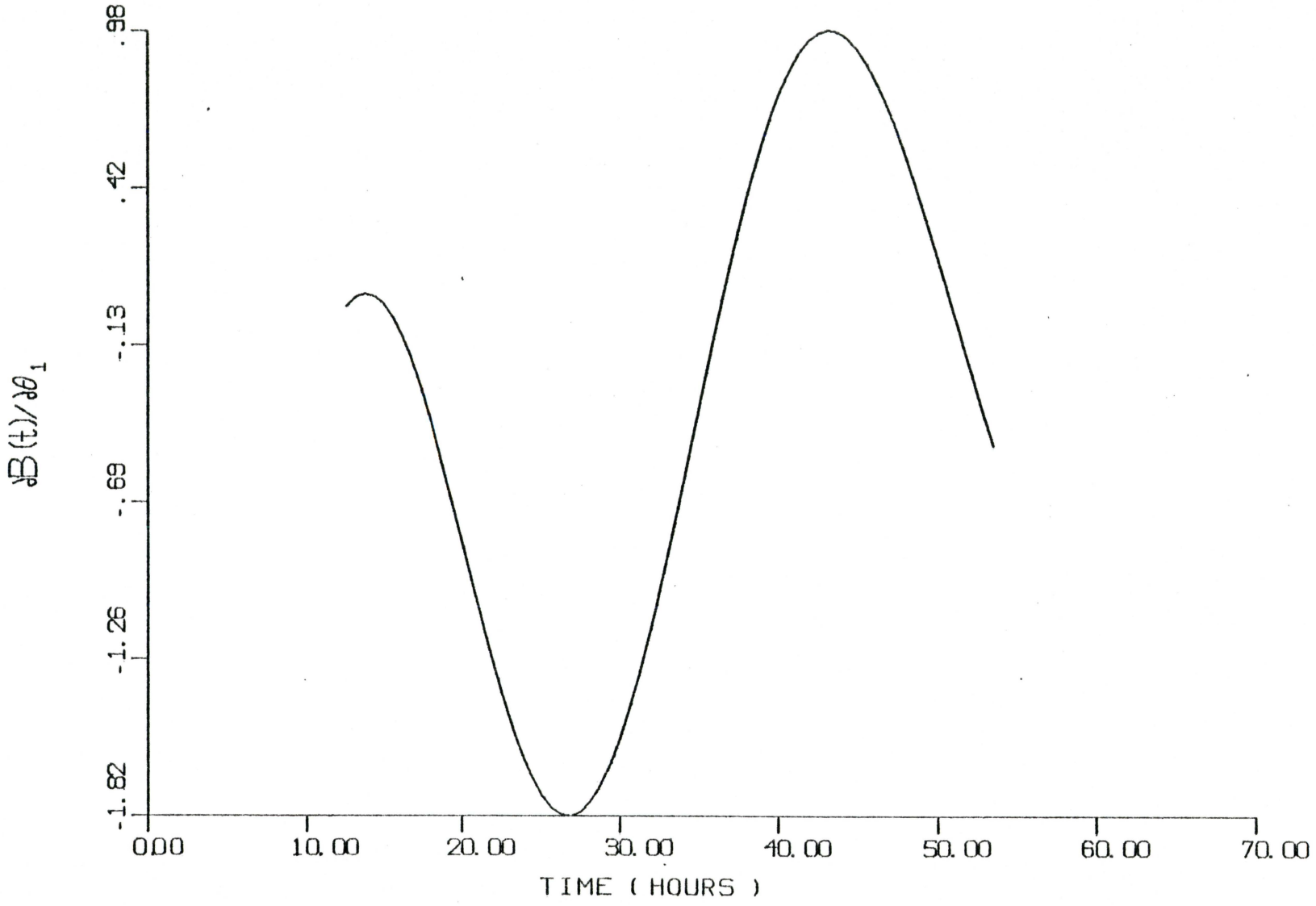

Fig. III-12. SENSITIVITY ANALYSIS OF σ_x

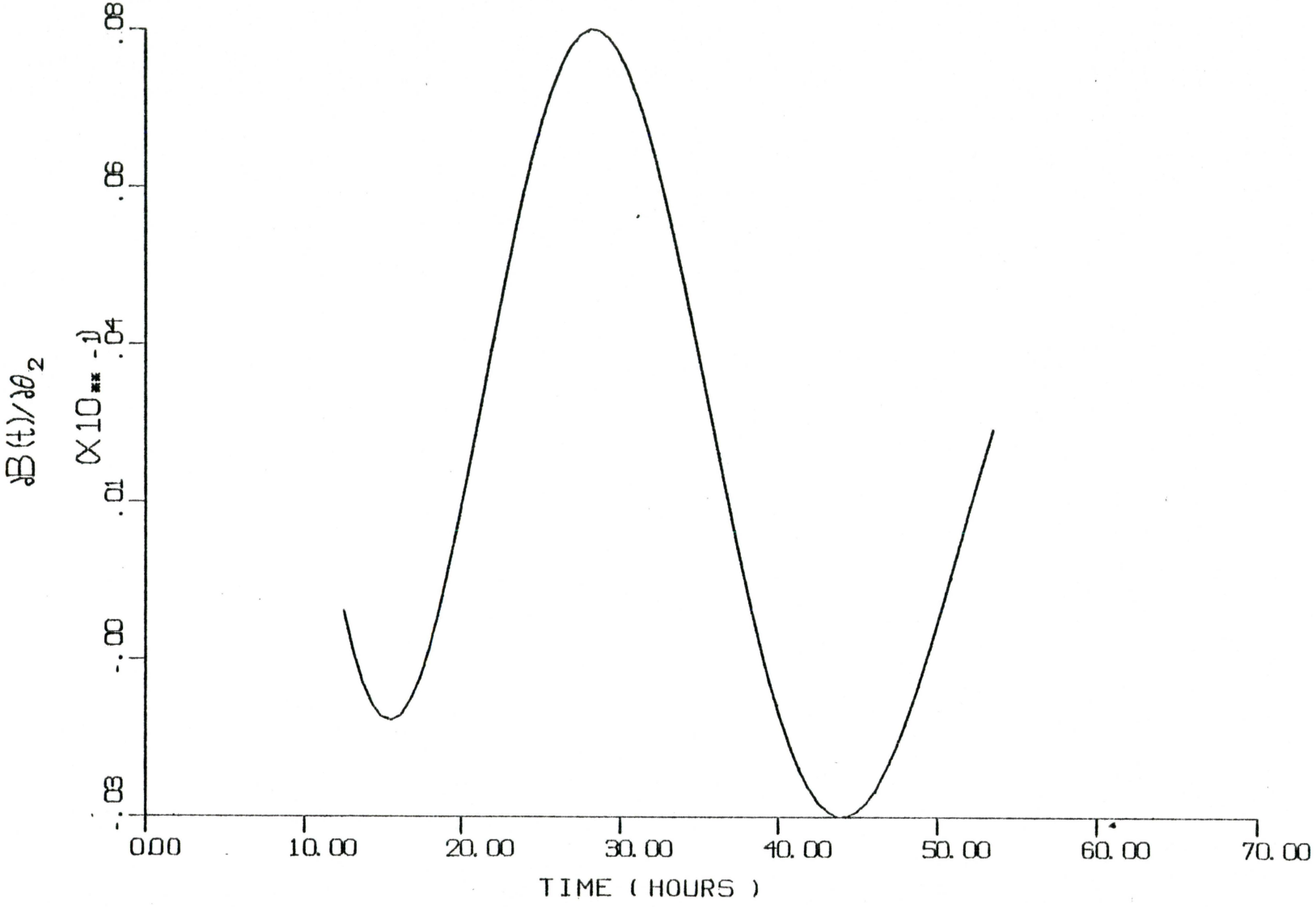

Fig. III-13. SENSITIVITY ANALYSIS OF D

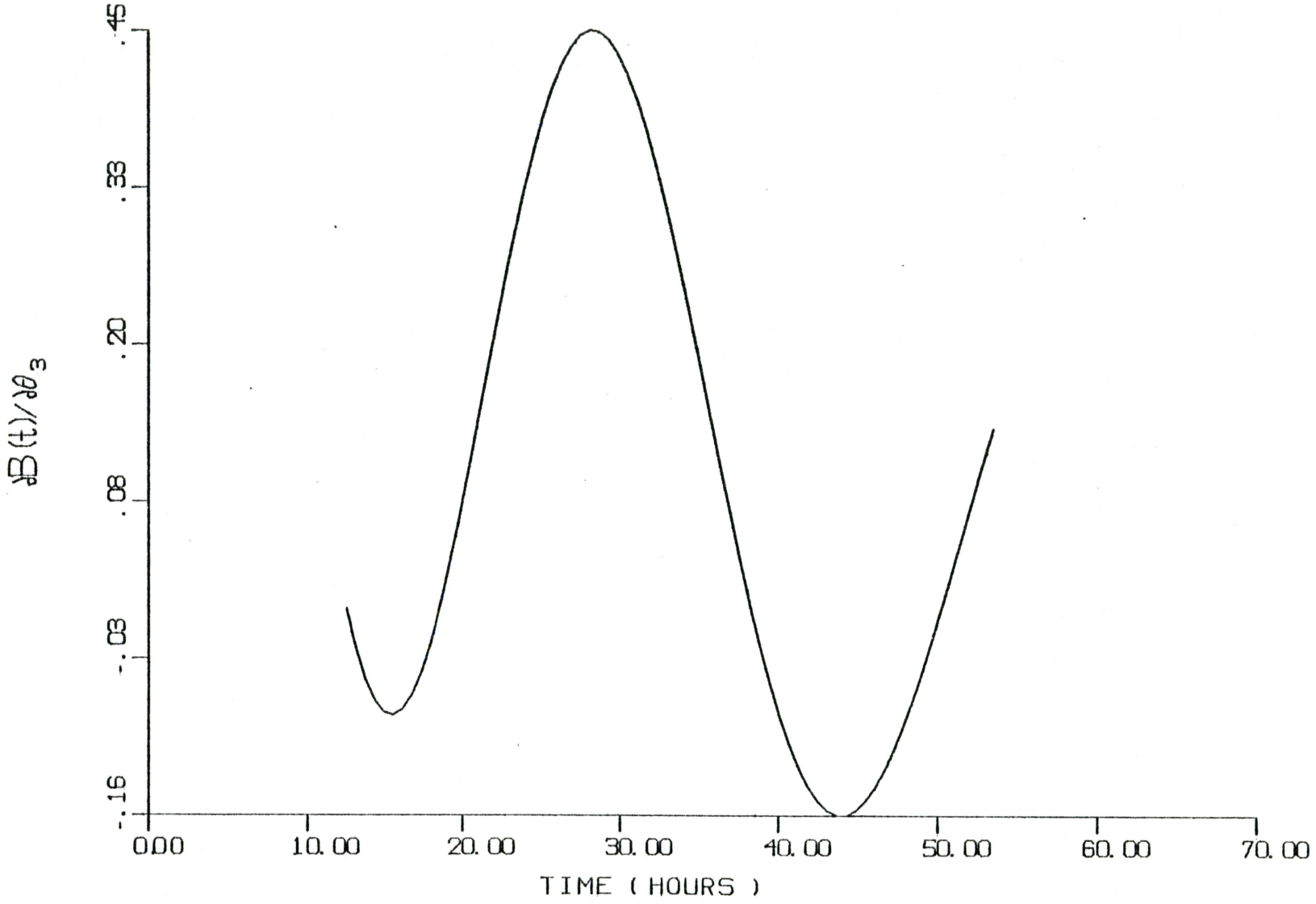

Fig. III-14. SENSITIVITY ANALYSIS OF α

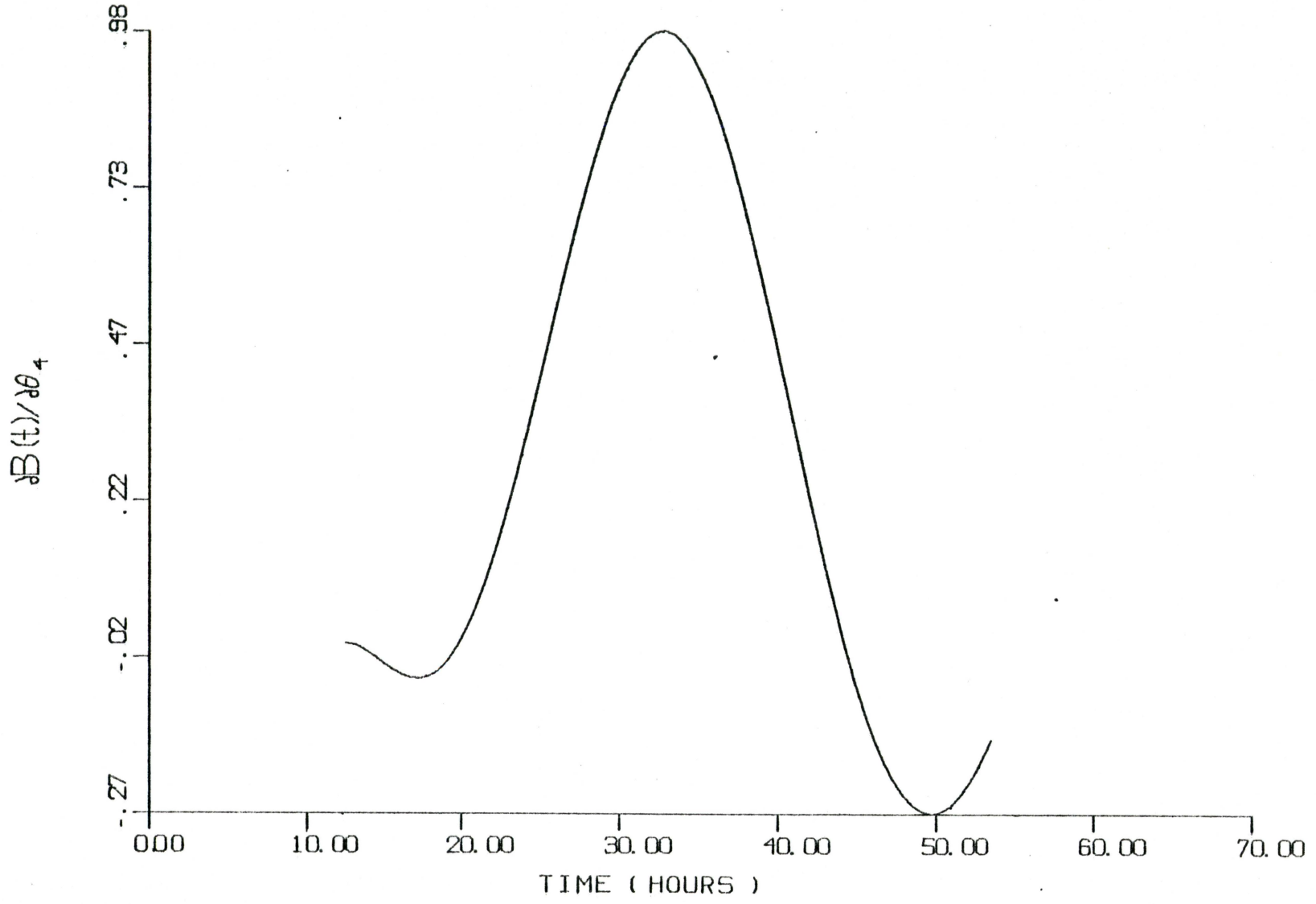

Fig. III-15. SENSITIVITY ANALYSIS OF Σ_f

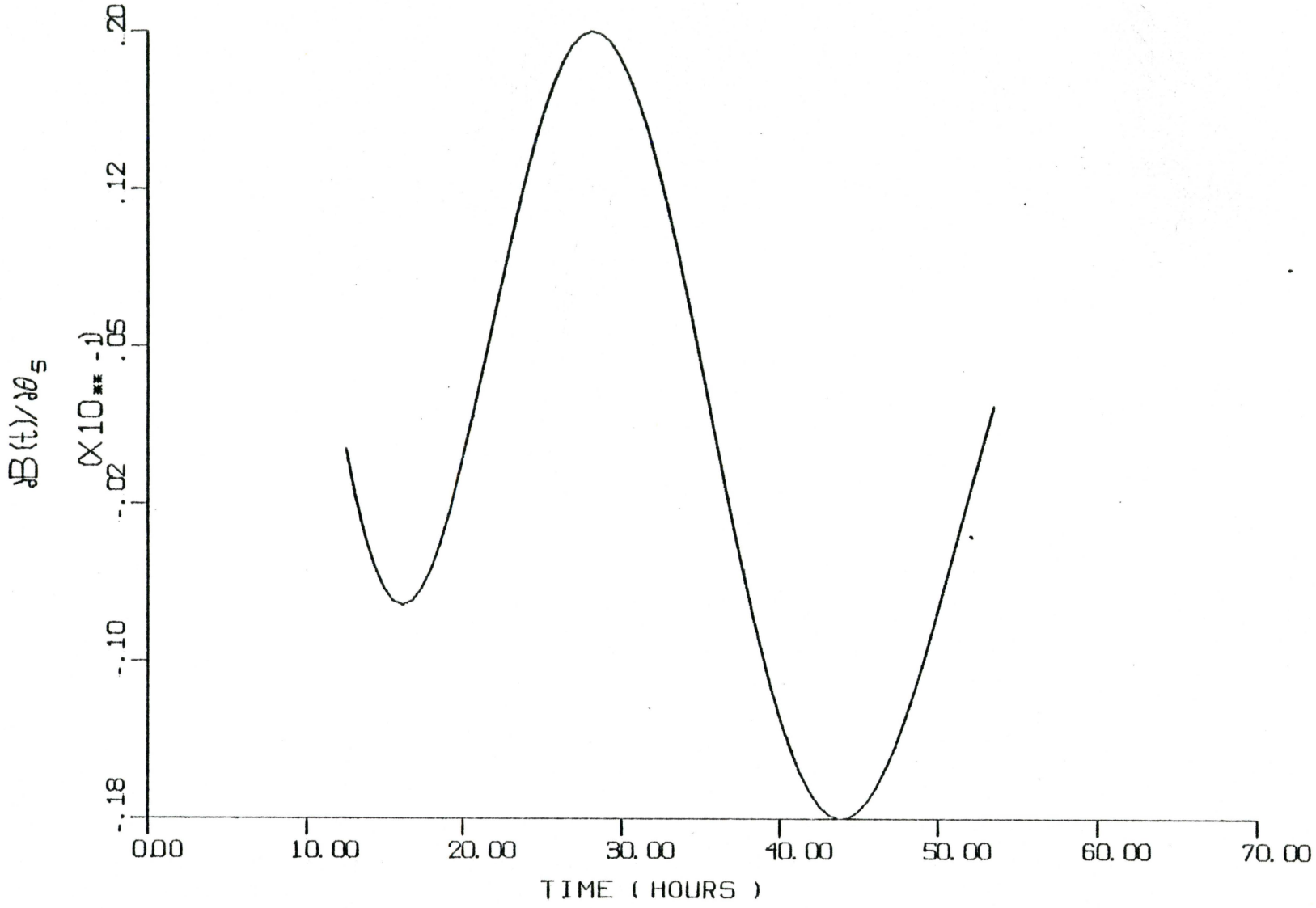

Fig. III-16. SENSITIVITY ANALYSIS OF γ_x

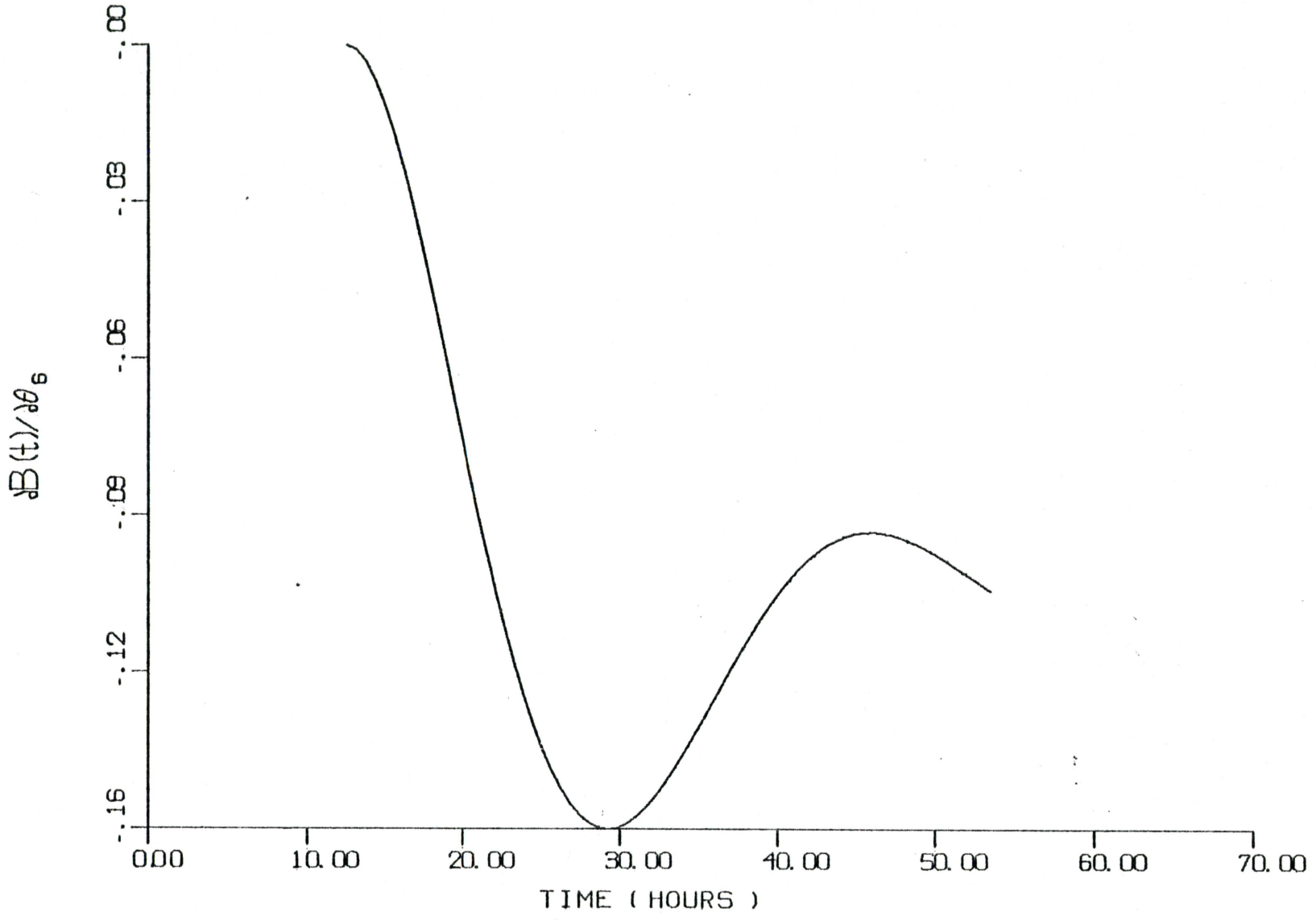

Fig. III-17. SENSITIVITY ANALYSIS OF γ_I

the only two terms that changed from the previous optimum values. For this unconstrained search γ_x was equal to 0.0005, an 83% change, and γ_1 was 0.046, a 24% change from the initial one group estimates. The chi-square fit for these parameters was 3.19 and the oscillation produced is shown in Fig. (III-18).

The oscillation produced in Fig. (III-18) came closer then initial estimates to matching the first half cycle of the plant data, especially the amplitude. However there resulted a sacrifice in the period of this oscillation and a overdamping of the response. For simulation times longer than were examined, this oscillation would die much too rapidly for practical considerations.

When comparing the respective sensitivity analysis plots between the linear and the nonlinear models, a phase shift in period was noticed between the first three plots of each model. An unconstrained optimization attempt was next performed while varying only these three parameters: σ_x, D, and α. This was attempted in order to compensate for the incorrect period of the linear model. It was also suspected that there was a competing process between correcting the amplitude against correcting the period. This attempt yielded surprisingly good results. The correct period was

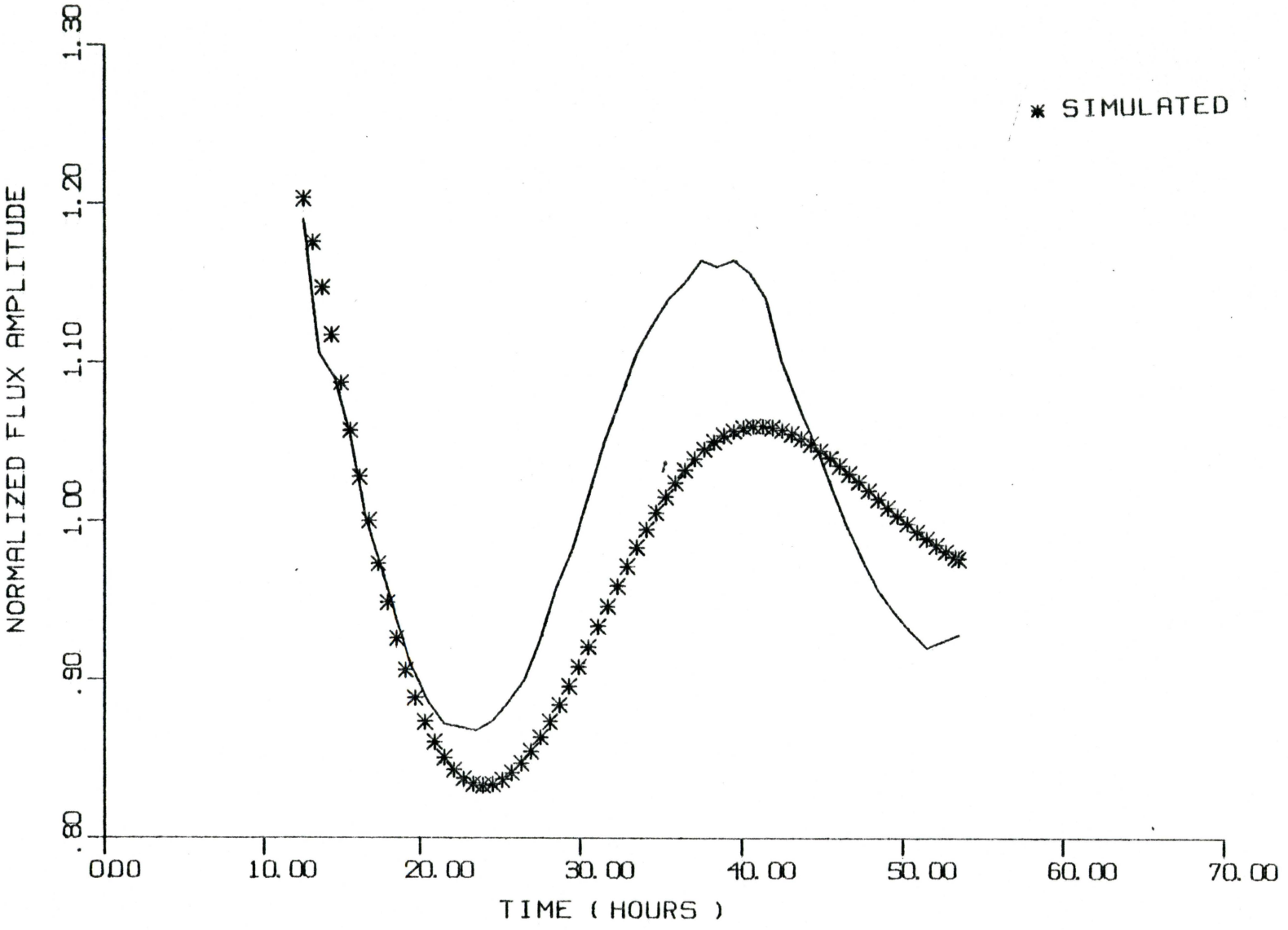

Fig. III-18 OPTIMUM LINEAR FIT (UNCONSTRAINED)

obtained and the chi-square fit was reduced to 1.86. The resulting simulation is shown in Fig. (III-19). The final values for the three parameters varied were:

$$\sigma_x = 3.91 \times 10^{-18} \text{ cm}^2 ,$$

$$D = .458 \text{ cm} ,$$

and $$\alpha = 5.64 \times 10^{-16} \text{ cm}^2 \cdot \text{sec}$$

while other values remained at their one group estimates.

The next attempt proved fruitless at varying the last three parameters Σ_f, γ_x , and γ_l while keeping the first three parameters at the above values. No reduction in the chi-square fit was obtained while keeping these last three parameter values positive.

The concern of the starting point for the linear model being fixed at time 12.5 hours can now be addressed. The linear model was only examined for the response predicted after pertubation, not during the time of the perturbation. The optimization process for the linear model worked very well for fitting the linear model oscillation against the actual oscillation; however, it could not correct for the

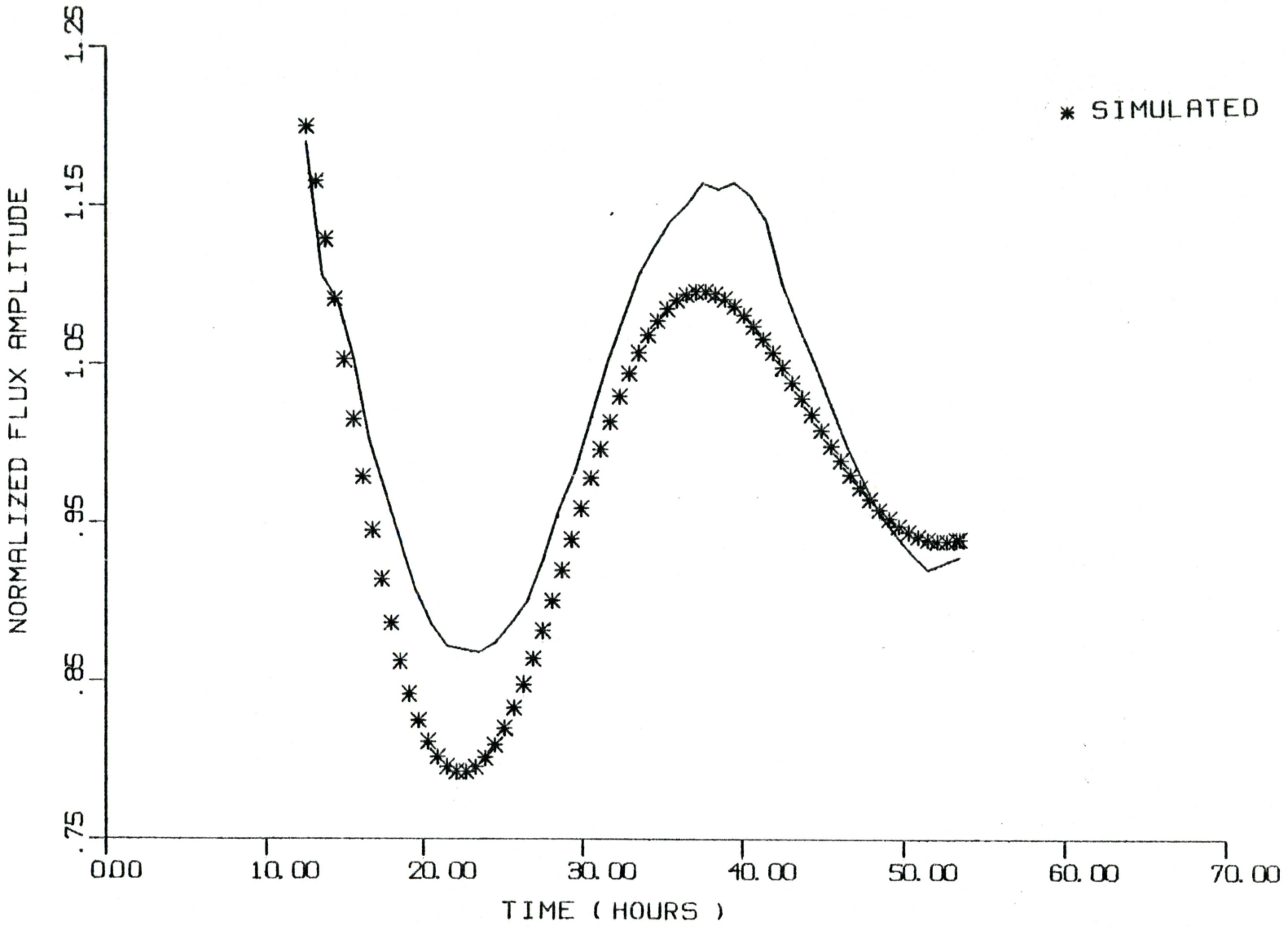

Fig. III-19 THREE PARAMETER OPTIMIZATION

starting point which was fixed due to the zero initial conditions. The correct values at time 12.5 hours for the nonlinear model were not necessarily the correct values for the linear model for the same time because of the differences in the two models and the wide variance in parameter values.

In an attempt to correct for the offset produced from the initial conditions, the nonlinear model was run with each iteration using the optimum values obtained from the linear model. This iterative process is shown in Fig. (III-20). The linear model was then optimized with these new initial conditions. This iterative process was continued until no significant change was noticed in the starting conditions. The final values for the starting conditions were found to be

$$A(12.5) = -0.0788 \quad ,$$

$$B(12.5) = 0.0677 \quad ,$$

and

$$C(12.5) = -0.0383 \quad .$$

The resulting simulation of the linear model with the corrected initial conditions is shown in Fig. (III-21). The

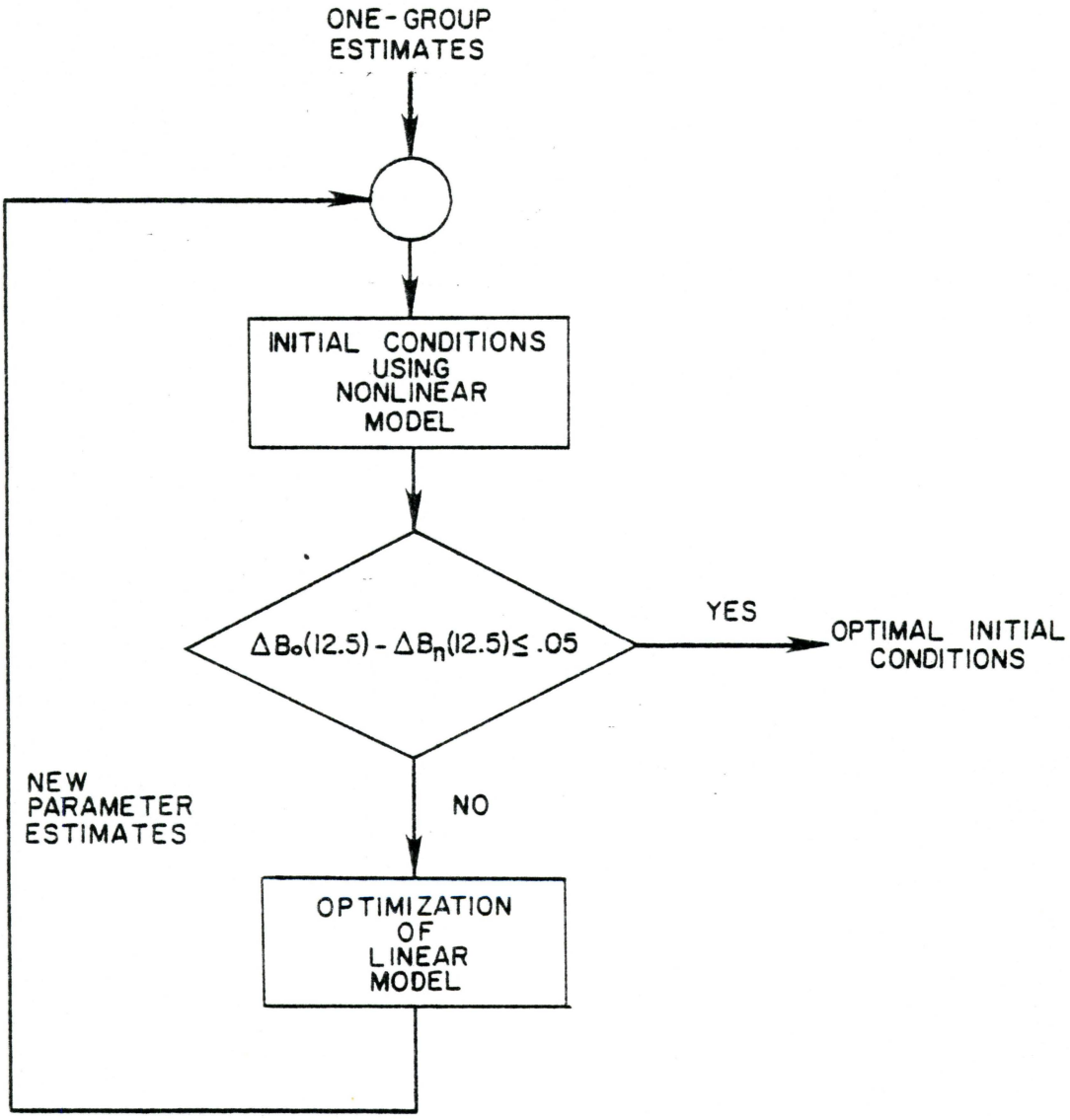

FIG. III-20 OPTIMIZATION FOR INITIAL CONDITIONS

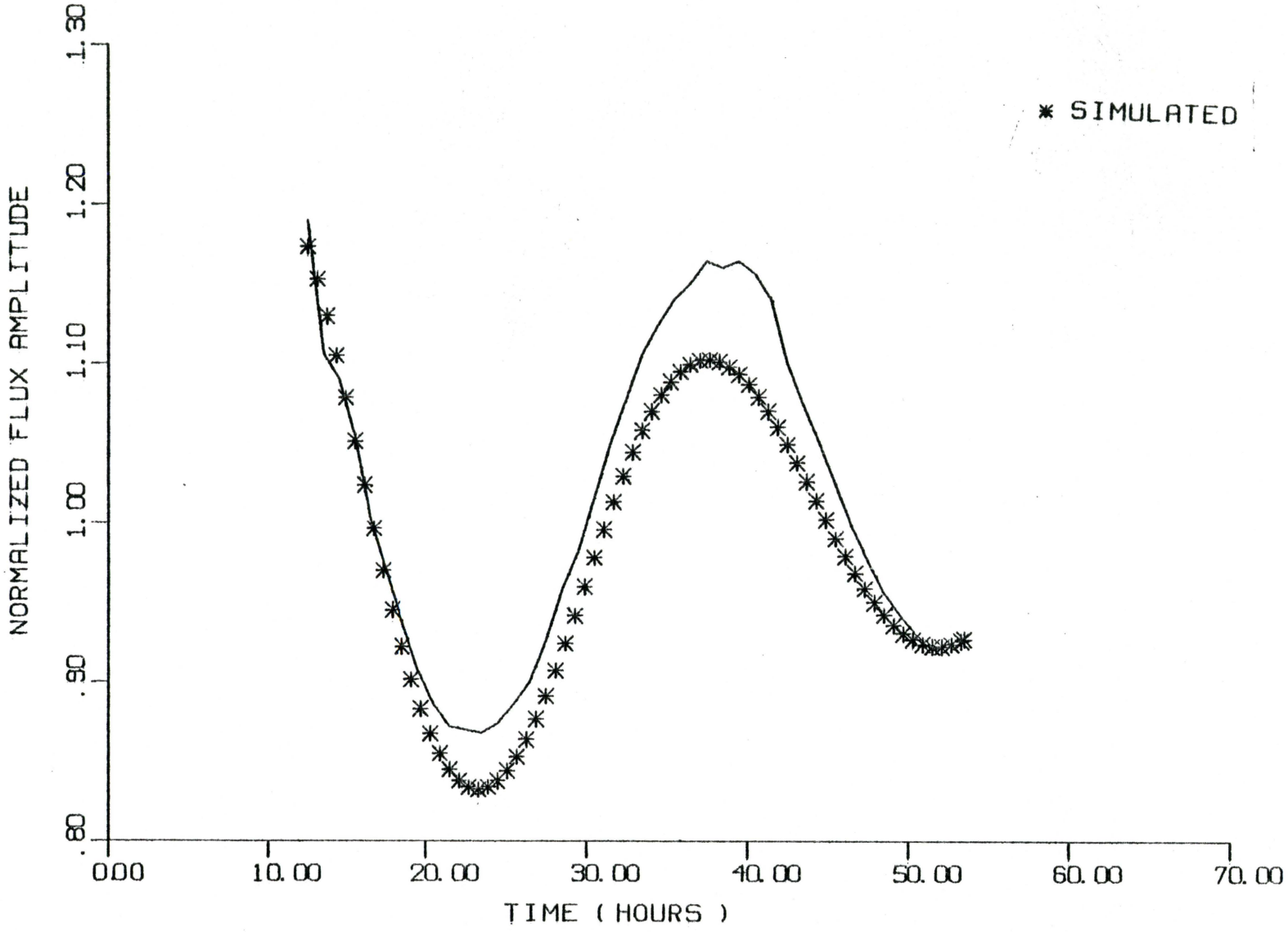

Fig. III-21 OPTIMUM CORRECTED LINEAR FIT

chi-square fit for this response was 1.04, a 50% increase from the nonlinear optimum fit. The values for this optimum point, which can be considered global, are listed in Table (III-3).

Since temperature feedback is the dominating effect in determining system stability (23), α was varied while the other parameters were kept at the values used in the above simulation, Fig. (III-21). The transition to stability, the stable oscillation, was found to occur when α was equal to 4.6E-16 $cm^2 \cdot sec$. Increasing the temperature feedback further resulted in additional damping of the response. The period at this point was 31 hours, precisely that obtained by Canosa (24). The stable oscillation for the nonlinear model at the same thermal flux level was found to be approximately 27 hours by Kisner (1).

The linearized xenon equations are used principally for investigations of stability. Variations in the flux have a strong influence as to whether a system is stable. The simulation of the linear model was performed while varying the average steady state thermal flux and the power feedback coefficient to determine the stability zones of the model. Figure (III-22) presents the resulting stability map. The stability map compares very well with the stability curve

TABLE III-3

Linear Model Optimum Values (Global)

Parameter	Optimum Value	% Change
$\sigma_x \times 10^{18}$ (cm^2)	3.973	50.0
D (cm)	0.453	14.7
$\alpha \times 10^{16}$ $(cm^2 \cdot sec)$	5.633	54.7
Σ_f (cm^{-1})	0.173	8.1
γ_x	0.0037	23.3
γ_i	0.066	8.2

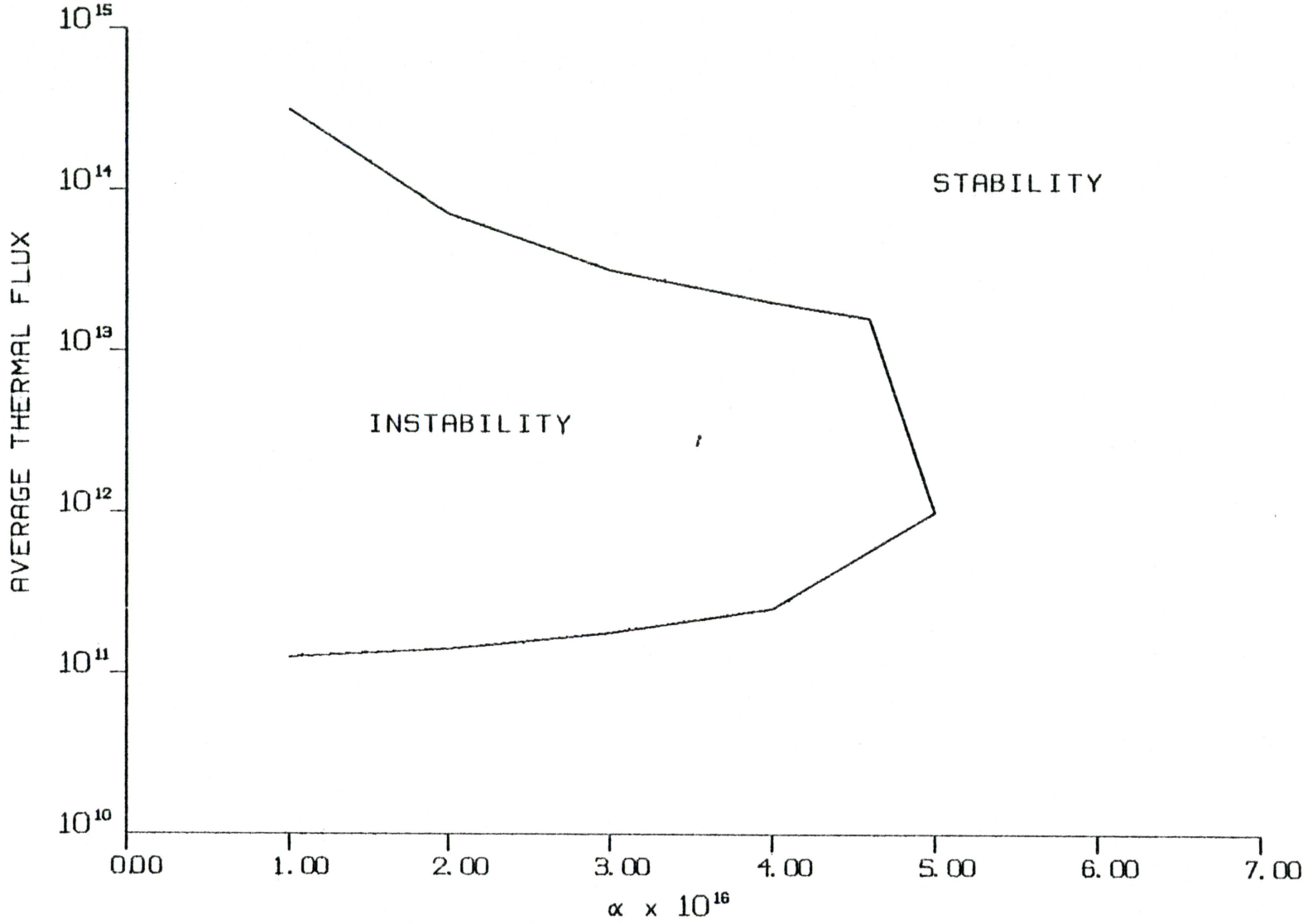

Fig. III-22 STABILITY ZONES OF LINEAR MODEL

for the nonlinear model (1) when the limit cycle (a constant cycle) is considered unstable. These results also are similiar to the stability regions predicted by Canosa except that the maximum power feedback coefficient for stability was to occur at a lower flux level in the linear model. This can be attributed to particular reactor parameters, especially reactor dimensions as mentioned by Canosa. Canosa does predict an unstable response for the initial one group estimate of α and thermal flux.

Chapter IV

CONCLUSIONS

4.1 SUMMARY OF RESULTS

The nonlinear xenon model was transformed into a linear model by linearizing the power reactivity feedback and xenon feedback terms. One purpose of this work was to examine the effects that this would produce. The advantages of working with a linear model for control applications are numerous. A linear system representation is greatly simplified by the use of Laplace transforms and frequency domain techniques which are the basic methods in classical control systems analysis.

Linearizing the two terms mentioned above produced a noticeable change in the accuracy of the pericd and drastic differences in the amplitude of oscillation for one group estimates as can be noticed when comparing Figs. (III-2) to (III-10). In fact, the linear model is unstable at the one-group estimates as compared to a stable response from the nonlinear model. A summary of results obtained are presented in Table (IV-1). Even when the linear model was stable the amplitude of oscillation was approximately three times larger but produced an acceptable pericd. Every attempt to reduce the amplitude resulted in a response similiar to Fig. (III-18), a highly overdamped system.

TABLE IV-1

Summary of Results

	Period (Hours)	χ^2
Exact (Diffusion Theory)	30.0	---
Initial Nonlinear Model	28.5	0.7082
20% Variation in Nonlinear Model	28.3	0.6995
Global Nonlinear Model	28.0	0.6951
Initial Linear Model	31.5	36.24
20% Variation in Linear Model	33.0	3.53
Global Linear Model	28.5	1.048

The competing effects for stability are xenon burnup (destabilizing) and reactivity feedback (stabilizing). The greatest variance in the sensitivity oscillations was in the xenon cross section as can be seen in Fig. (III-12). This most likely resulted in the linear model being unstable at the initial one group estimates. Linearizing the xenon burnup increases this term's dominance in the linear model and results in a decrease in damping. However the response of the power feedback was similiar for both models.

4.2 CONCLUSIONS

The most significant flaw of the linear model was the dependance on the nonlinear model for initial conditions. The large area of instability as shown in Fig. (III-22) was also very detrimental to the linear model. The initial unstable response predicted by the linear model with the one group estimates is completely unacceptable. The feasibility of this model will depend on large values of the power feedback coefficient to produce a stable response.

4.3 RECOMMENDATIONS

The initial one group estimates were a good approximation for the nonlinear model with optimum values. However for the linear model these estimates were unsatisfactory.

Since the nonlinear model initially provided an excellent response with one group diffusion theory estimates this model would be expected to provide equally good results for general simulation purposes and is recommended over the linear model.

The linear model has serious restrictions that seriously hinder its utilization. The major one is that initial conditions for this system must depend on external sources (i.e., the nonlinear model). This is in contrast to the nonlinear system that can inherently produce its own perturbation. The large variance in parameter values from diffusion theory estimates also prevents this model from applications for on-line simulation.

The final fit of the linear model was, however, acceptable. The iterative search between the two models for the initial conditions made the linear model unattractive even though the model would be ideal for reactor control applications. Further investigation is suggested into the linear model so that it can incorporate a perturbation by overcoming the computer application problem of dividing by zero. If this could be eliminated than the linear model could become divorced from the nonlinear system.

One method of accomplishing this could be to rewrite the linear model computer program in FORTRAN instead of CSMP. Besides simplifying the program this would enable conditional statements to equate a term to zero if it is being divided by zero.

Other possible recommendations to improve the response obtained from the linear model are:

1. Increasing the number of regions of the simulated core.

2. Use multigroup diffusion theory as opposed to single group.

3. Represent the spatial distribution with a different series reprsentation.

Appendix A

GRADIENT OPTIMIZATION METHOD

The maximum likelihood equation developed by Cnega (16) was

$$\frac{\partial \chi^2}{\partial \theta_j} = \frac{\partial \chi^2}{\partial \psi_i^c} \frac{\partial \psi_i^c}{\partial A} \frac{\partial A}{\partial V} \frac{\partial V}{\partial B} \frac{\partial B}{\partial \theta_j} \tag{A.1}$$

where ψ_i^c is the calculated relative flux and $\partial B/\partial \theta_j$ are the sensitivity equations. The best estimates for θ_j were obtained when the norm of the gradient was a minimum, i.e.,

$$\text{Min} \left\{ \left\| \nabla \chi^2 \right\| \right\} = \text{Min} \left\{ \sqrt{\sum_1^6 \left[\frac{\partial \chi}{\partial \theta_j} \right]^2} \right\} \text{ for all } \theta_j, \; j=1, \cdots 6. \tag{A.2}$$

As can be seen, minimizing the value of Eq. (A.1) will minimize the value the Eq. (A.2). However, since Eq. (A.1) is a function of the sensitivity equations, then minimizing the value of the sensitivity equations minimizes the value of the gradient.

Before each simulation new constants are calculated since they are all functions of θ_j, which is being varied. If these new values reduce the amplitude of A(t), B(t), and

C(t), then their partial derivatives will be reduced, i.e., if A(t), B(t), and C(t) aren't changing, then their partials (the rate of change) are equal to zero. This produces a flat response having a perfect gradient of the chi-square fit. The only values that A(t), B(t), and C(t) can reduce to is zero. This argument holds for the linear system just as well as for the nonlinear system.

Appendix B

NONLINEAR SENSITIVITY EQUATIONS

The nonlinear system sensitivity equations are

$$\frac{\partial A}{\partial \theta_1} = - \frac{\partial A}{\partial v} \frac{1}{\theta_1} \left[\frac{1}{8\ B(t)} + v \right] ,$$

$$\frac{\partial A}{\partial \theta_2} = \frac{\partial A}{\partial v} \left[\frac{(45/8\ \pi^3/H^2\ D^\circ \theta_2)}{(8\ X_\circ\ \sigma_x^\circ \theta_1\ B(t))} \right] ,$$

$$\frac{\partial A}{\partial \theta_3} = \frac{\partial A}{\partial v} \left[\frac{(7\ \phi_\circ \Sigma_a\ \alpha^\circ\ \theta_3)}{(8\ X_\circ\ \sigma_x^\circ \theta_1\ B(t))} \right] ,$$

$$\frac{\partial A}{\partial \theta_4} = \frac{\partial A}{\partial \theta_5} = \frac{\partial A}{\partial \theta_6} = 0 ,$$

$$\frac{d}{dt}\left[\frac{\partial C}{\partial \theta_j}\right] = c11 \frac{\partial A}{\partial \theta_j} - \lambda_1 \frac{\partial C}{\partial \theta_j} ,$$

and

$$\frac{d}{dt}\left[\frac{\partial B}{\partial \theta_j}\right] = b11 \frac{\partial A}{\partial \theta_j} + b12 \frac{\partial C}{\partial \theta_j} - \lambda_1 \frac{\partial B}{\partial \theta_j} - b14 \left\{ 2/3 \left[\frac{\partial A}{\partial \theta_j} + \frac{\partial B}{\partial \theta_j} \right] + \pi/4 \left[A \frac{\partial B}{\partial \theta_j} + B \frac{\partial A}{\partial \theta_j} \right] \right\} - b14\, \delta_{j1} \left[2/3\ (A+B) + \pi/4\ AB \right] .$$

The δ_{jl} represents the Kronecker delta and

$j = 1, 2, 3, \ldots 6.$

Appendix C

LINEAR SENSITIVITY EQUATIONS

The linear system sensitivity equations are

$$\frac{d}{dt}\left[\frac{\partial \Delta C}{\partial \theta_j}\right] = z1\,\frac{\partial \Delta B}{\partial \theta_j} + \frac{(z2 + z3)\;\Delta B}{e6^2\, B_o^4\,(e1^2 + e4\; B_o^2)} - \lambda_1\,\frac{\partial \Delta C}{\partial \theta_j}\quad ,$$

$$z1 = \frac{-c11\;e1(e1^2 + e4\;B_o^2)^{1/2} + c11\;e1}{e6\;B_o^2(e1^2 + e4\;B_o^2)^{1/2}}\quad ,$$

$$z2 = e6\;B_o^2(e1^2 + e4\;B_o^2)^{1/2}\frac{\partial}{\partial \theta_j}$$

$$x\left[-c11\;e1(e1^2 + e4\;B^2)^{1/2} + c11\;e1^2\right]\quad ,$$

$$z3 = c11\;e1(e1^2 + e4\;B_o^2)^{1/2} + c11\;e1^2$$

$$x\;\frac{\partial}{\partial \theta_j}\left[e6\;B_o^2(e1 + e4\;B_o^2)^{1/2}\right]\quad ,$$

$$\frac{d}{dt}\left[\frac{\partial \Delta B}{\partial \theta_j}\right] = b12\,\frac{\partial \Delta C}{\partial \theta_j} - y1 - y2 - B(y3 - y4) - y5\,\frac{\partial \Delta B}{\partial \theta_j},$$

$$y1 = (\lambda_x + 2/3\ b14)\frac{\partial \Delta B}{\partial \theta_j} + B\ \frac{\partial}{\partial \theta_j}(\lambda_x + 2/3\ b14)$$

$$y2 = \frac{(b11 - 2/3\ b14)\ e1}{B_o e6}\ \frac{\partial \Delta B}{\partial \theta_j}$$

$$+ \Delta B\left\{\left[(B_o^2 e6\ \partial/\partial\theta_j\ (b11 - 2/3\ b14)\ e1\right] - e1(b11 - 2/3\ b14)\ \partial/\partial\theta_j\ (B_o^2 e6)\right\} \Big/ (B_o^2 e6)^2 ,$$

$$y3 = e6(e1^2 + e4\ B^2)^{1/2}\ \partial/\partial\theta_j (y6\ e4) - e4\ y6\ \partial/\partial\theta_j\left[e6(e1^2 + e4\ B_o^2)^{1/2}\right] / e6^2(e1^2 + e4\ B_o^2),$$

$$y4 = \frac{\left\{e6\ B_o^2 \partial/\partial\theta_j\left[(e1^2 + e4\ B_o^2)^{1/2}(b11 - 2/3\ b14)\right] - (e1^2 + e4\ B_o^2)^{1/2}(b11 - 2/3\ b14)\ \partial/\partial\theta_j\ (e6\ B_o^2)\right\}}{(e6^2\ B_o^4)} ,$$

$$y5 = \frac{y6\ e4}{e6(e1^2 + e4\ B_o^2)^{1/2}} - \frac{(e1^2 + e4\ B_o^2)^{1/2}(b11 - 2/3\ b14)}{e6\ B_o^2},$$

and

$$y6 = (b11 - 2/3\ b14 - \pi/4\ b14\ B) .$$

Appendix D

THE HOOKE AND JEEVES METHOD

The Hooke and Jeeves' method (19), which was developed in 1961, attempts to find the most profitable search directions to minimize the chi-square fit even while constraints are applied. The initial values of the variables are called the initial base point, b_j and initial step sizes, h_j, for the respective variables. The function is evaluated at the initial base points then each variable is incremented plus or minus h_j for a particular simulation. If a move is a success (reducing the chi-square fit), then that variable is replaced with its new increment. If a move is a failure then that variable is left unchanged. This is continued until all the variables have been incremented around that particular base point.

A pattern, or leapfrog move, attempts to speed up the search by jumping base points in the direction which has led to a decrease in the chi-square fit. If this results in a failure, then the new base point is the old base point replaced with the newly incremented variables. When changing base points does not result in any future success, the step sizes are reduced.

REFERENCES

1. Kisner, R. A., "A Two Point Variational Model For The Reactor Core Subject To Xenon-Induced Flux Oscillations", M.S. Thesis, Virginia Polytechnic Institute and State University, 1976.

2. Duke Power Company, Oconee Nuclear Stations Unit II Startup Report, Docket No. 50-270, (1974).

3. Duderstadt, J.J. and L.J. Hamilton, Nuclear Reactor Analysis, John Wiley and Sons, Inc., N.Y., 1976.

4. Raymond, W. J., "Presurized Water Reactor Startup Testing," M.S. Thesis, Virginia Polytechnic Institute and State University, 1975.

5. Lamarsh, J. R., Introduction To Nuclear Engineering, Wesley Publishing Company, Reading, Massachusetts, 1977.

6. Onega, R. J., An Introduction to Fission Reactor Theory, University publications, Blacksburg, Virginia, 1975.

7. Foster, A. R. and R. L. Wright, Basic Nuclear Engineering, Allyn and Bacon, Inc., Boston, 1973

8. Bell, G. and S. Glasstone, Nuclear Reactor Theory, Van Nostrand Reinholt Co., N.Y., 1970.

9. Rydin, R. A., "A Lambda-Mode Evaluation of Time Step Corrections in Xenon Oscillation Simulation," Atomkernenergie(ATKE) Bd. 28, 1976.

10. Rydin, R. A., Nuclear Reactor Theory and Design, University Publications, Blacksburg, Virginia, 1977.

11. Rydin, R. A., "Higher Flux Mode Effects in Xenon Spatial Oscillations," Nucl. Sci. Engr., 50, 147-152, 1973.

12. Chernick, J., "The Dynamics of a Xenon-Controlled Reactor," Nucl. Sci. Engr., 8, 233, 1960.

13. Chernick, J., Lellouche, G., and Wollman, W., "The Effect of Temperature on Xenon Instability," Nucl. Sci. Engr., 10, 120, 1961.

14. Onega, R. J. and R. A. Kisner, "An Axial Xenon Oscillation Model," Annals of Nuclear Energy, 5, 13-19, 1977.

15. Frogner, B., Friedlander, B., and H. Rao, "Methods for Identification of Dynamic Systems," Nucl. Sci. Engr., 64, 644-656, 1977.

16. Onega, R. J. and R. A. Kisner, "Parameter Identification for Spatial Xenon Transient Analysis and Control," to be published in Annals of Nuclear Energy.

17. Wismer, D. A. and R. Chattergy, Introduction to Nonlinear Optimization, North-Holland, New York, 1978.

18. Cooper, L. and D. Steinberg, Introduction to Methods of Optimization, W. B. Saunders Company, Philadelphia, 1970.

19. Walsh, G. R., Methods of Optimization, John Wiley and Sons, New York, 1977.

20. Speckhart, F. H. and W. L. Green, A Guide to using CSMP - The Continuous System Modeling Program, Prentice-Hall, New Jersey, 1976.

21. Continuous System Modeling Program III (CSMP III), Program Reference Manual, GH20-0367-4, IBM Corp., White Planes, N.Y. 1972.

22. Brogan, W. L., Modern Control Theory, Quantum, New York, 1974.

23. Stacey, W. M., Space-Time Nuclear Reactor Kinetics, Academic Press, New York, 1969.

24. Canosa, J. and H. Brooks, "Xenon-Induced Oscillations," Nucl. Sci. Engr., 26, 237, 1966.

25. Carnahan, B., Luther, H., and J. Wilkes, Applied Numerical Methods, John Wiley & Sons, New York, (1969).

The vita has been removed from the scanned document

PARAMETER OPTIMIZATION OF THE NONLINEAR AND LINEAR XENON OSCILLATION MODELS

by

Vincent Joseph Mastroianni Jr.

(ABSTRACT)

The object of this work was to develop a linear two-point reactor model frcm an existing nonlinear model and determine optimum parameters for both models in comparison to actual plant data. The importance of keeping the nonlinearity to accurately describe the xenon oscillation problem was also examined. The best chi-square fit to the actual test data was established as the guiding criterion.

The nonlinear model initially produced an excellent chi-square fit of 0.708 against plant data. This value could only be reduced through parameter variation to 0.695, approximately 2%. The linear model resulted in a diverging oscillation at the initial one group estimates. Linearizing the oscillatory behavior of the xenon burnup coefficient was attributed to the decrease in the stability of the model. The major flaw of the linear model was the dependence on the nonlinear model for initial condtions.